

# **Treatment of textile wastewater using electrochemical oxidation**

**SARRA JEBALI**

*Dissertation submitted to Escola Superior de Tecnologia e Gestão de Bragança to obtain  
the Degree of Master in Chemical Engineering under the scope  
of the double diploma with Université Libre de Tunis*

Supervised by

**António Manuel Coelho Lino Peres**

**Ana Sofia Fajardo**

**Ana Cristina Veloso**

**Abdeslem Hamrouni**

*This dissertation includes the comments mentioned by the Jury*

**Bragança**

**2025**

## **Dedication**

This work is dedicated with all my heart to my cherished grandparents. To **Kheiria Wahada**, whose gentle spirit and quiet strength continue to guide me, and to **Mokhtar Lasfar**, a symbol of resilience and kindness. To my dear, long-departed grandfather, **Ali Jebali**, whose memory I hold close every day—your absence is deeply felt. And to **Hlima Boukari**, whose warmth and love have been a constant support.

To my extraordinary parents, **Mounir Jebali** and **Faten Lasfar**, whose sacrifices and unwavering belief in me have been the foundation of every success I've achieved. Your unconditional love has carried me through every high and low, and I am forever grateful for the values and strength you have instilled in me.

To my sisters, **Mariem Jebali** and **Rahma Chaabane**, my confidantes and lifelong cheerleaders. You've been my rock, my laughter in moments of stress, and my closest friends through it all.

To my friends, who have filled this journey with laughter, shared dreams, and moments of joy that I will cherish forever.

This dissertation stands as a tribute to each of you, a reflection of the love, faith, and inspiration you have poured into my life. It is for you, and because of you, that I am here today.

## **Acknowledgment**

I would like to express my deepest gratitude to my esteemed Professors, whose guidance, support, and expertise have been invaluable throughout the journey of completing this seminar.

To Professor António Manuel Coelho Lino PERES, your insightful feedback and encouragement have helped shape my research and expand my understanding of the subject matter. Your dedication to excellence in teaching and research has been a constant source of inspiration.

To Professor Ana Sofia FAJARDO, I am truly grateful for your mentorship and encouragement. Your passion for academia and commitment to student success have been instrumental in my academic growth and development.

To Professor Ana Cristina VELOSO, your expertise and guidance have been instrumental in shaping the direction of my research. Your unwavering support and constructive criticism have been invaluable in refining my ideas and methodology.

To Professor Abdessalem Hamrouni, I extend my sincere appreciation for your support and encouragement throughout this dissertation. Your expertise has enriched my research and broadened my perspective.

I am deeply grateful for the opportunity to learn from such distinguished scholars, and I am honored to have had the privilege of working under your mentorship. Thank you for your unwavering support, guidance, and dedication to academic excellence.

Your involvement has been crucial to my journey, and I genuinely value your commitment.

I'm truly grateful to have conducted my experiments for this dissertation at two wonderful institutions in Portugal: The Instituto Politécnico de Bragança (IPB) and the Instituto Politécnico de Coimbra (IPC). Their invaluable resources and support were absolutely crucial to the successful completion of this work.

Thank you,  
Sarra JEBALI.

## Abstract

Water pollution is a significant environmental issue, driven by contaminants from industrial, agricultural, and domestic sources. Recently, persistent organic compounds have emerged as major pollutants, prompting the need for more advanced treatment solutions. Although traditional methods such as filtration, adsorption, and biological processes have been applied, they often suffer from low efficiency, high energy costs, and the risk of secondary pollution. Therefore, electrochemical methods have gained attention as efficient alternatives, offering controlled and verifiable oxidation and reduction reactions for pollutant degradation, with the added benefits of versatility and minimal secondary waste. In this study, electrochemical oxidation was implemented to treat water pollutants, evaluating the performance of different anode materials boron-doped diamond (BDD), titanium coated with iridium dioxide (Ti/IrO<sub>2</sub>), and titanium coated with ruthenium dioxide (Ti/RuO<sub>2</sub>). In addition to electrode material, the effects of several key operational parameters were investigated, including current density, inter-electrode distance, mixing rate, and initial dye concentration, in order to determine their impact on color and chemical oxygen demand (COD) removal efficiencies. The BDD anode demonstrated superior performance, achieving 100% color removal consistently across all current densities, presenting optimal results. A current density of 0.06 A/cm<sup>2</sup> was selected as it offers ideal balance in terms of color and COD removal efficiency as well as cost-effectiveness, with COD removal reaching 30.3%. The operational parameters were systematically optimized to enhance the efficiency of the electrochemical oxidation process, and an inter-electrode distance of 0.5 cm was found to be the most effective, yielding the highest COD removal of  $35.7 \pm 0.56$  (95% CI: [35.6, 35.9]); a mixing rate of 250 rpm led to a COD removal of  $68.8 \pm 0.67$  (95% CI: [68.7, 68.9]); and an initial methylene blue concentration of 50 ppm resulted in the highest COD removal, reaching  $80.9 \pm 0.03$  (95% CI: [80.7, 81.1]). These findings emphasize the potential of electrochemical oxidation, particularly using BDD anodes under optimized conditions, for efficient and sustainable water treatment.

**Keywords:** Electrochemical oxidation, Boron-doped diamond, Color removal, COD removal, Methylene blue, Current density, wastewater treatment.

## Resumo

A poluição da água é um problema ambiental significativo, impulsionado por contaminantes provenientes de fontes industriais, agrícolas e domésticas. Recentemente, compostos orgânicos persistentes surgiram como poluentes principais, exigindo a necessidade de soluções de tratamento mais avançadas. Embora métodos tradicionais como filtração, adsorção e processos biológicos tenham sido aplicados, estes frequentemente sofrem de baixa eficiência, altos custos energéticos e risco de poluição secundária. Portanto, métodos eletroquímicos têm ganhado atenção como alternativas eficientes, oferecendo reações de oxidação e redução controladas e verificáveis para a degradação de poluentes, com os benefícios adicionais de versatilidade e resíduos secundários mínimos. Neste estudo, a oxidação eletroquímica foi implementada para tratar poluentes da água, avaliando o desempenho de diferentes materiais de ânodo : diamante dopado com boro (BDD), titânio revestido com dióxido de irídio (Ti/IrO<sub>2</sub>) e titânio revestido com dióxido de rutênio (Ti/RuO<sub>2</sub>). Além do material do eletrodo, os efeitos de vários parâmetros operacionais chave foram investigados, incluindo densidade de corrente, distância entre eletrodos, taxa de agitação e concentração inicial do corante, a fim de determinar seu impacto na remoção de cor e na eficiência de remoção da demanda química de oxigênio (DQO). O ânodo de BDD demonstrou desempenho superior, alcançando 100% de remoção de cor consistentemente em todas as densidades de corrente, apresentando resultados ótimos. Uma densidade de corrente de 0,06 A/cm<sup>2</sup> foi selecionada por oferecer o equilíbrio ideal em termos de eficiência de remoção de cor e DQO, bem como em relação ao custo-benefício, com a remoção de DQO alcançando 30.3%. Os parâmetros operacionais foram sistematicamente otimizados para aumentar a eficiência do processo de oxidação eletroquímica, e uma distância entre eletrodos de 0.5 cm foi considerada a mais eficaz, proporcionando a maior remoção de DQO de  $35.7 \pm 0.56$  (IC 95%: [35.6, 35.9]); uma taxa de agitação de 250 rpm levou a uma remoção de DQO de  $68.8 \pm 0.67$  (IC 95%: [68.7, 68.9]); e uma concentração inicial de azul de metileno de 50 ppm resultou na maior remoção de DQO, atingindo  $80.96 \pm 0.03$  (IC 95%: [80.7, 81.1]). Esses resultados enfatizam o potencial da oxidação eletroquímica, particularmente utilizando ânodos de BDD sob condições otimizadas, para um tratamento de água eficiente e sustentável.

**Palavras-chave** : Oxidação eletroquímica, Diamante dopado com boro, Remoção de cor, Remoção de DQO, Azul de metileno, Densidade de corrente, Tratamento de águas residuais.

## Table of contents

Dedication .....	i
Acknowledgment.....	ii
Abstract .....	iii
Resumo.....	iv
Table of contents.....	v
List of figures .....	vii
List of tables .....	ix
List of abbreviations .....	x
CHAPTER I INTRODUCTION .....	1
I.1 Framework .....	2
I.2 Objectives .....	3
CHAPTER II THEORETICAL BACKGROUND AND LITERATURE REVIEW .....	5
II. 1 Textile wastewater and treatment processes.....	6
II.1.1 Dyes .....	6
II.1.2 Overview of the conventional treatment methods for textile wastewater.....	8
II.1.3 Biological methods .....	10
II.1.4 Physical methods.....	10
II.1.5 Advanced textile industry wastewater processes.....	11
II.1.5.1 Electrochemical advanced processes.....	12
II.1.5.2 Anodic materials.....	14
II.2 Portuguese legislation for wastewater treatment.....	16
CHAPTER III MATERIALS AND METHODS.....	17
III.1.1 Methylene blue solution preparation .....	18
III.1.2 Electrochemical setup .....	19
III.1.3 Analysis of the removal of methylene blue.....	21
III.2 Analytical techniques .....	22
III.2.1 pH .....	22
III.2.2 Conductivity.....	23
III.2.3 Absorbance (UV-Vis).....	24
III.2.4 Chemical oxygen demand (COD).....	25
III.3 Industrial parameters .....	26
III.3.1 Energy consumption.....	26
III.3.2 Current efficiency .....	26
CHAPTER IV RESULTS AND DISCUSSION .....	29

IV.1 Characterization of the synthetic effluent .....	30
IV.2 Effect of the current density on color and COD removal.....	30
IV.2.1 Effect of the current density on color removal.....	30
IV.2.2 Effect of current density on chemical oxygen demand (COD).....	33
IV.3 Effect of inter-electrode distance on color and COD removal.....	37
IV.3.1 Effect of inter-electrode distance on color removal.....	37
IV.3.2 Effect of inter-electrode distance on COD removal.....	38
IV.4 Effect of the mixing rate on color and COD removal .....	41
IV.4.1 Effect of the mixing rate on color removal .....	41
IV.4.2 Effect of the mixing rate on COD .....	42
IV.5 Effect of the concentration of methylene blue on color and COD removal .....	44
IV.5.1 Effect of the concentration of methylene blue on color removal .....	44
IV.5.2 Effect of the concentration of methylene blue on COD removal .....	45
CHAPTER V CONCLUSIONS AND PERSPECTIVES .....	48
References.....	51

## List of figures

**Figure II.1:** Different possible dye degradation techniques [30].

**Figure III.1:** Chemical formula of methylene blue.

**Figure III.2:** UV-vis spectra of MB.

**Figure III.3:** Electrochemical setup (a) and electrodes with acrylic spacers covered with Teflon (b).

**Figure III.4:** Multimeter used for pH and conductivity measurements.

**Figure III.5:** UV-Vis spectrophotometer.

**Figure IV.1:** Effect of current density on color removal and on chemical oxygen demand (COD). (a): Effect of current density on color removal using BDD anode, (b): Effect of current density on color removal using Ti/IrO<sub>2</sub> anode, (c): Effect of current density on color removal using Ti/RuO<sub>2</sub>, (d): Effect of current density on chemical oxygen demand (COD) for all the anodes (d). The COD obtained for all electrodes is at 360 minutes.

**Figure IV.2:** The energy consumption (EC) and the current efficiency (CE) for all the electrodes at different current densities. Bars correspond to EC and dots correspond to CE.

**Figure IV.3:** Effect of different inter-electrode distance on color and COD removal. (a): Effect of different inter-electrode distance on color removal. (b): Effect of different inter-electrode distance on COD removal. The COD obtained is at 360 minutes.

**Figure IV.4:** The energy consumption and current efficiency at different inter-electrode distances. Bars correspond to EC and dots correspond to CE.

**Figure IV.5:** Effect of the mixing rate on color and COD removal. (a): Effect of the mixing rate on color removal. (b): Effect of the mixing rate on COD removal. The COD obtained is at 360 minutes.

**Figure IV.6:** The energy consumption and current efficiency for the electrodes at different mixing rates. Bars correspond to EC and dots correspond to CE.

**Figure IV. 7:** Effect of the initial concentration of methylene blue on color and COD removal. (a): Effect of the initial concentration of methylene blue on color removal. (b): Effect of the initial concentration of methylene blue on COD removal. The COD obtained is at 360 minutes.

**Figure IV.8:** The energy consumption and current efficiency at different initial methylene blue concentrations. Bars correspond to EC and dots correspond to CE.

## **List of tables**

**Table II.1:** Classification and characterisation of dyes [26, 27].

**Table II.2:** Different possible dye degradation techniques [30] [Adapted]

**Table II.3:** Biological methods, advantages and disadvantages [32].

**Table II.4:** Physical methods, advantages and disadvantages [33].

**Table II.5:** Advanced wastewater treatment processes [33].

**Table III.1:** Dilution plan for BDD anode.

**Table IV.1:** pH and conductivity evolution for the electrodes at different current densities. The conductivity and pH obtained for all electrodes is at 360 minutes.

**Table IV.2:** calculated Ohmic resistance for the different inter-electrode distances.

## **List of abbreviations**

**BDD:** Boron-doped diamond

**BNC:** Bacterial nanocellulose

**BOD:** Biochemical oxygen demand

**CE:** Current Efficiency

**COD:** Chemical oxygen demand

**DSA:** Dimensional stable anodes

**EAOP:** Electrochemical advanced oxidation process

**EC:** Energy Consumption

**EO:** Electrochemical oxidation

**H<sub>2</sub>SO<sub>4</sub>:** Sulfuric acid

**HTC:** High-temperature combustion

**K<sub>2</sub>Cr<sub>2</sub>O<sub>7</sub>:** Potassium dichromate

**Na<sub>2</sub>SO<sub>4</sub>:** Sodium sulfate

**NDIR:** Non-dispersive infrared

**TDS:** Total dissolved solids

**Ti/ IrO<sub>2</sub>:** Titanium Iridium Dioxide

**Ti/RuO<sub>2</sub>:** Titanium Ruthenium Dioxide

**TSS:** Total suspended solids

**UV-Vis:** Ultraviolet Visible

# **CHAPTER I**

## **INTRODUCTION**

## **I.1 Framework**

Modernization and population growth have led to a rising demand for beauty and color. To fulfill this demand, industries such as textiles, leather, paper, and plastics extensively use dyes to color their products, consuming significant amounts of water. However, 10–15% of dyes are lost into waste streams during production and discharged into the environment in large quantities. The untreated release of these effluents into water systems causes ecosystem damage, water shortages, and quality degradation [1-4]. Water pollution and scarcity, driven by hazardous and persistent pollutants in wastewater, pose a severe threat to millions of people and represent one of the most critical environmental challenges of this century [5-8].

The contamination of water bodies by synthetic organic substances is a critical issue, as it can lead to severe health problems such as cancer, genetic mutations [9], organ dysfunction, and cyanosis [10]. Water pollution caused by synthetic dyes from textile industries represents a significant environmental challenge. In addition to dyes, textile wastewater contains a variety of organic and inorganic pollutants, including finishing chemicals, surfactants, inhibitors, active substances, chlorine compounds, salts, phosphates, dissolved solids, and total suspended solids (TSS) [11].

The discharge of these effluents into aquatic environments leads to significant pollution, adversely affecting aquatic organisms and altering key parameters such as biochemical oxygen demand (BOD), chemical oxygen demand (COD), total dissolved solids (TDS), total suspended solids (TSS), and pH levels [12]. The impact on natural streams and aesthetic concerns has driven the development of new water framework directives [13, 14], prompting the scientific community to explore innovative solutions for effectively treating industrial effluents [15].

The primary goal of treating wastewater effluents is to ensure high water quality and protect the health of ecosystems. Numerous methods have been suggested for treating dye-laden wastewater, including catalytic oxidation, membrane filtration, coagulation, flocculation, adsorption, and biological techniques [16-21]. However, many commercial treatment technologies face challenges such as lengthy treatment durations, sludge disposal problems, reliance on chemicals, and the generation of secondary pollution [22, 23].

## I.2 Objectives

This research evaluated the performance of boron-doped diamond (BDD), titanium coated with ruthenium dioxide (Ti/RuO<sub>2</sub>), and titanium coated with iridium dioxide (Ti/IrO<sub>2</sub>) anodes, using sodium sulfate (Na<sub>2</sub>SO<sub>4</sub>) as the supporting electrolyte. The approach of this study begins with preparing synthetic solution that mimics the composition of textile wastewater. To treat the synthetic wastewater through systematic experimentation and meticulous analysis, encompassing the exploration of electrode material variations, inter-electrode spacing adjustments, optimal current density determination, and stirring rate evaluations, and the initial concentration of pollutant, this research aims to refine treatment methodologies ensuring the determination of the best operational conditions meanwhile attaining a cost-effective system. To achieve this, a series of experiments was carried out, during which each operational parameter was varied. By conducting experiments in a controlled environment, with only one parameter altered at a time, we seek to understand the behavior and interactions of experimental parameters that influence the treatment process. Each experiment was conducted separately, with only one parameter altered at a time. This systematic shuffling of conditions allows for a comprehensive understanding of how each factor contributes to the overall performance needed to optimize the electrolytic treatment. Different electrode materials were tested to compare their efficiency in promoting electrochemical degradation. Current density was adjusted across a defined range to determine the most effective level for generating oxidizing species without incurring excessive energy costs. Inter-electrode distances were modified step-by-step to evaluate their impact on electric field distribution and resulting electrochemical reaction rates. Stirring rates were varied to analyze their role in enhancing mass transport within the electrolyte solution. Furthermore, the initial concentration of methylene blue was included as a critical parameter, as it directly influences both the reaction kinetics and the pollutant load in the system and to assess the availability of sufficient reactive species per unit of dye molecule. To evaluate pollutant degradation, color removal was monitored at 0, 5, 15, 30, 90, 120, 180, 240, 300, and 360 min, using UV-Visible spectrophotometry at a wavelength of 663.5 nm, which corresponds to the maximum absorbance peak of methylene blue. The decrease in absorbance over time provided a quantitative measure of the dye's breakdown under various experimental conditions. In parallel, chemical oxygen demand (COD), an indicator of the organic content remaining in the solution, was determined before and after treatment, using a standard dichromate digestion method followed by spectrophotometric analysis at 600 nm, enabling an estimation of the mineralization degree of

the organic load. A key focus of the study was on the energy consumption (EC) and current efficiency (CE) of the system, as these are critical indicators of both economic and environmental viability. Lower EC and higher CE are essential for reducing operational costs and maximizing the effective use of electrical input, thereby improving the overall sustainability of electrochemical water treatment technologies. By studying each parameter individually and in combination, the goal of the research was identifying the most effective configuration of current density, inter-electrode distance, stirring rate, electrode material, and initial dye concentration to achieve maximum pollutant degradation. This involved determining how each variable influences color removal and COD reduction, with the aim of developing an electrochemical treatment process that balances high efficiency, energy savings, and minimal secondary pollution, while also ensuring reproducibility of results, long-term electrode stability.

## **CHAPTER II**

# **THEORETICAL BACKGROUND AND LITERATURE REVIEW**

## **II. 1 Textile wastewater and treatment processes**

### **II.1.1 Dyes**

Each year, approximately 1 million tons of dyes are produced from around 10,000 commercial dye types. Globally, dye manufacturing and dye-using industries generate an estimated 3,000 to 4,000 kilotons of wastewater annually. Among the various sources of dye wastewater, the textile industry is the largest contributor of about 54% of dye effluent polluting the environment. This accounts for more than half of the worldwide industrial dye effluent produced. The dyeing industry contributes up to 21% while the paper and pulp industry, tannery and paint industry, and dye manufacturing contributes up to 10%, 8% and 7% respectively to the overall through their various process activities [24].

Key dye-manufacturing countries play a significant role in global production. China leads with an annual dye production of approximately 300,000 tons, followed by India, which produces around 200,000 tonnes per year. Germany, a major European producer, contributes nearly 50,000 tonnes annually, while Spain, Italy, France, and England collectively produce around 80,000 tonnes. Japan and Pakistan also have substantial production capacities, each accounting for 30,000 tonnes annually [25].

Natural dyes offer several advantages over synthetic dyes, including non-toxicity, ease of extraction and purification, renewability, and minimal effluent generation. While reverting to natural dyes could be a more sustainable approach, their limitations hinder widespread industrial adoption. These drawbacks include the need of mordants to achieve effective bonding with fabrics, low shade reproducibility, and poor color fastness. Mordants are chemical binding agents that facilitate the attachment of natural dyes to fibers; however, many mordants are toxic and pose significant environmental risks, like synthetic dyes. In contrast, synthetic dyes consist of complex molecular structures that enhance their stability. They contain auxochromes and chromophores, which contribute to their water solubility and strong substrate affinity, leading to improved dye retention and coloration performance [26].

A report by the Central Pollution Control Board in India states there are about 1 million identified dyes and dye intermediates. Although dyes are categorized in various ways, as shown in table II.1, classifications based on their chemical properties and applications have become more prevalent.

Chemists often classify dyes based on the chromophoric groups in their molecular structures. Chromophores, which are electron-withdrawing groups, include C=C, C=N, C=O, N=N, NO<sub>2</sub>, and NO. Auxochromes, acting as electron-donating groups, include NHR, NH<sub>2</sub>, OH, NR<sub>2</sub>, COOH, SOH, and OCH<sub>3</sub>. Dyes are classified based on their chemical structure, bonding mechanism, source of raw materials, chemical composition, and industrial applications, as outlined in Table II.1. They can be categorized as either natural or synthetic, depending on their origin.

Natural dyes are derived from biological sources such as plants, with common examples including turmeric (*Curcuma longa*), onion (*Allium cepa*), and indigo (*Indigofera tinctoria*). Synthetic dyes, on the other hand, are chemically synthesized and widely utilized in various industries. Major classes of synthetic dyes include azo, disperse, acid, basic, direct, mordant, reactive, sulfur, and vat dyes. Among these, azo dyes represent the largest category, accounting for approximately 70% of global dye production and consumption [27].

**Table II.1:** Classification and characterisation of dyes [26, 27].

Dye Type	Water Solubility	Chromophoric Groups	Applications	Examples
<b>Acid</b>	Soluble	Azo, anthraquinone, azine, nitroso, triphenylmethane, xanthene, nitro	Food, silk, leather, wool, nylon, paper, cosmetics, printing ink, acrylics	Acid Yellow 36, Acid Orange 19
<b>Basic</b>	Soluble	Acridine, azo, oxazine, anthraquinone, azine, cyanine, thiazine, diazahemicyanine	Silk, wool, inks, medicine, paper, straw, tannin-mordant cotton, polyesters	Crystal Violet, Methylene Blue
<b>Azo</b>	A type of direct dye	Stilbene, pyrazoles, coumarin, anaphthalimides	Rayon, cotton, plastics, paints, acetate, cellulosic materials, detergents	Direct Red 88, Acid Orange 19
<b>Disperse</b>	Insoluble	Azo, anthraquinone, nitro, styryl, benzodifurandione	Polyester, nylon, plastic, cellulose acetate, acrylic fibers	Disperse Blue 27, Disperse Yellow 3

**Table II.1: Continuation.**

<b>Dye Type</b>	<b>Water Solubility</b>	<b>Chromophoric Groups</b>	<b>Applications</b>	<b>Examples</b>
<b>Direct</b>	Soluble	Polyazo compounds, stilbenes, oxazines, phthalocyanines	Cotton, rayon, paper, leather, nylon, wool, silk, cellulose, fibers, linen	Direct Orange 39, Direct Blue 15
<b>Fluorescent Brighteners</b>	Mostly soluble (some insoluble)	Naphthylamides, stilbene, coumarin, pyrazoles	All fibers, oils, paints, plastics, soaps, detergents	4, 4'-bis(ethoxycarbonyl vinyl) stilbene
<b>Mordant</b>	Soluble	Anthraquinone and azo	Anodized aluminum, wool, leather	Mordant Blue 3
<b>Oxidation Bases</b>	–	Aniline black and indeterminate structures	Cotton, fur, hair	Direct Blue
<b>Reactive</b>	Soluble	Azo, anthraquinone, triphenylmethane, formazan, phthalocyanine, oxazine	Cotton, wool, yarn, silk, painting, polychromatic printing	Reactive Blue 5
<b>Vat</b>	Insoluble (soluble in alkali)	Anthraquinone (polycyclic quinones), indigoids, carbazole	Cotton, cellulosic fibers, polyester-cotton, rayon, wool	Vat Orange 1, Indigo (Vat Blue 1)
<b>Solvent</b>	Insoluble (nonpolar or slightly polar)	Azo, anthraquinone, phthalocyanine, triphenylmethane	Plastics, gasoline, lubricants, oils, waxes	Solvent Red 24, Solvent Yellow 124
<b>Sulfur</b>	Insoluble	Nitro and amino groups	Cotton, rayon, polyamide fibers, silk, leather, paper	Sulfur Black 1, Indophenol

### II.1.2 Overview of the conventional treatment methods for textile wastewater

The International Dye Industry Wastewater Discharge Quality Standards have implemented the Zero Discharge of Hazardous Chemicals Programme (ZDHC) [28]. Thus, textile industries are obligated to minimize the use of harmful

carcinogenic, mutagenic, and allergenic chemicals for textile dyeing purposes. The detoxification of textile sewage not only includes abolition of colors but also requires degradation and mineralization of the dye substrate. Furthermore, several features, such as composition of wastewater, nature of dye, environmental fate, handling, running costs, technical influence, and economic viability of dye removal process require attention [29].

To address these challenges an extensive variety of technologies have been developed to achieve satisfactory and acceptable quality level of water by degradation or removal of synthetic dye products as shown in Tab.II.2.

**Tab II.2:** Different possible dye degradation techniques [30] [Adapted]

<b>Type</b>	<b>Category</b>	<b>Specific technique</b>
<b>Traditional Techniques</b>	Physical treatment	Coagulation, flocculation, adsorption, ion-exchange
	Biological treatment	Bacterial decolorization
<b>Advanced techniques</b>	Chemical treatment (advanced oxidation processes)	Ozonation, Fenton's process, photochemical process, irradiation, electrochemical process
	Biological treatment	Fungal Decolorization, other Prokaryotic decolorization, bacterial consortium, enzymatic decolorization, phytoremediation
	Physical treatment	Membrane filtration
	Combinatorial treatment	Biological-Chemical combination: Anaerobic-Aerobic followed by Fenton's process
	Nanotechnology	Nanomaterial-enhanced adsorption

Traditional wastewater treatment solutions have already been tested to eliminate chemical compounds present in textile wastewaters, namely dyes:

### II.1.3 Biological methods

The biological cleaning of toxic contaminants from industrial wastewater, using microorganisms, mainly microalgae and bacteria, and in some cases, fungi, yeasts, and enzymes, during aerobic and anaerobic process, decolorizes textile-coloring compounds into simple, non-toxic chemical compounds. Other biological methods include adsorption by microbial biomass, algae degradation, enzyme degradation, fungal cultures, and microbial cultures as shown in table II.3 illustrating their merits and demerits [31].

**Table II.3:** Biological methods, advantages and disadvantages [32].

<b>Methods</b>	<b>Advantages</b>	<b>Disadvantages</b>
<b>Enzyme degradation</b>	It is nontoxic, reusable, inexpensive and highly efficient	Unreliable enzyme production
<b>Adsorption by microbial biomass</b>	Some dyes have high affinity that allows them to bind with microbial biomass	Effective for limited number dyes
<b>Aerobic-anaerobic method</b>	Cheap and effective for decolorizing a wide variety of dye	Produces sludge, yields methane and hydrogen sulphide as by-products
<b>Microbial cultures</b>	It takes between 24-30 hours to decolorize	Not effective for all dyes

### II.1.4 Physical methods

Based on the mass transfer mechanism, various physical approaches such as adsorption, ion exchange, and membrane filtration are used to treat dye-containing wastewater. Several other methods, such as chemical precipitation, ion exchange, membrane filtration, and coagulation-flocculation, are employed for dye and heavy metals removal from the environment. However, these methods involve the use of numerous chemicals while producing toxic sludge as illustrated in table II.4 [31].

**Table II.4:** Physical methods, advantages and disadvantages [33].

<b>Methods</b>	<b>Advantages</b>	<b>Disadvantages</b>
<b>Adsorption by activated carbon</b>	Excellent ability to remove a wide variety of dyes. Adsorbent regeneration	Expensive
<b>Ion exchange</b>	Regeneration prevents loss absorbent. High quality water output	Effective for few numbers of dyes
<b>Electrocoagulation</b>	Inexpensive and feasible	Production of large sludge
<b>Membrane Filtration</b>	Effective for all dye type, water recovery and reuse	Expensive to setup, generate concentrated sludge
<b>Reverse osmosis</b>	Production of clean water, useful for water recycling and effective for wide variety of dye	Requires high pressure and expensive

### **II.1.5 Advanced textile industry wastewater processes**

The previous discussed methods have proven not to be efficient in completely removing the dyes from water streams due to their refractory characteristics, which make them resistant to biodegradation when introduced into an aquatic habitat [34]. Dyes, their intermediates, and degradation products may alter water transparency and gas solubility, which threaten marine life [35].

Advanced treatment processes have been researched for environmental protection, such as Fenton oxidation, the ultraviolet (UV) irradiation and the ozone (O<sub>3</sub>) as depicted in table II.5 [36, 37].

**Table II.5:** Advanced wastewater treatment processes [33].

<b>Method</b>	<b>Function</b>
<b>Fenton Oxidation</b>	Uses hydrogen peroxide (H <sub>2</sub> O <sub>2</sub> ) and iron (Fe <sup>2+</sup> ) catalysts to generate hydroxyl radicals (•OH) that aggressively decompose complex organic pollutants, including dyes. Effective but produces iron sludge and requires pH control.
<b>Ultraviolet (UV) Irradiation</b>	Uses UV light to disinfect water by damaging the DNA of bacteria, viruses, and other microorganisms. Can also help degrade some organic pollutants but is mainly used for microbial inactivation.
<b>Ozone (O<sub>3</sub>) Treatment</b>	A powerful oxidizing process that destroys pathogens and breaks down organic pollutants, including dyes and pharmaceuticals. Leaves no harmful residues but requires ozone generation equipment.

These processes have grown in popularity in recent decades, from ninety articles annually in 2000 to more than a thousand pieces in 2019, inspired by the desire to treat a wide range of environmental pollutants [38, 39]. These processes are compact, easily automatable, chemical-free technologies to treat wastewater effluents [40, 41], and most importantly, they are especially effective at eliminating organic contaminants that are resistant to traditional methods of treatment [42].

### **II.1.5.1 Electrochemical advanced processes**

Electrochemistry is a discipline of chemistry that investigates the interaction of electrical and chemical processes. It is named after the study of electron mobility in an oxidation-reduction reaction. It is a fundamental multidisciplinary field with applications in a wide variety of physical, chemical, and biological domains. Electrochemical reactions are chemical processes that generate electrical currents and chemical reactions that are initiated by the flow of electricity. In a chemical reaction, including electron transfer, one species obtains one or more electrons while the other loses one or more electrons. Oxidation refers to species

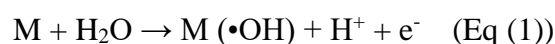
that lose electrons, whereas reduction refers to those that gain electrons. Both processes must take place synchronously [42].

Over the past decade, electrochemical treatment technologies, including electro-flotation, electro-coagulation, and electro-oxidation, have gained significant attention for their efficiency, robustness, and cost-effectiveness. These methods present a promising alternative for treating various types of industrial wastewater [43-45].

Electrochemical technology has recently emerged as a highly effective method for treating dye-contaminated wastewater, offering a high decolorization rate and efficient removal of chemical oxygen demand (COD) [46, 47]. Electrochemical oxidation techniques, including direct and indirect oxidation, have been applied to treat dye-laden wastewater [48–58].

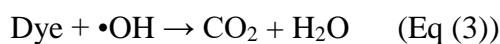
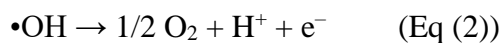
The most common electrochemical advanced oxidation process (EAOP) is electrochemical oxidation (EO) which has been effectively used to lower the organic load and toxicity of wastewater. EO occurs via two main pathways: either direct anodic oxidation, where the oxidation of pollutants is by transferring electrons directly to the electrode surface (Eq (1)), or indirect oxidation, with electrogenerated potent oxidizing hydroxyl radicals ( $\bullet\text{OH}$ ) formed by water discharge at the anode surface (M) (Eq. (1)) [59]. These radicals are capable of efficiently degrading dyes and organic compounds until they mineralize, converting the organic contaminants, pathogens, and refractory chemicals into non-hazardous species (low molecular weight, rapidly biodegradable compounds, and/or carbon dioxide and water) resulting in the destruction of the chromophoric groups responsible for the color of the dye [60].

The decomposition of water molecules on the surface of the anode (M) is exemplified in equation (1) [61, 62].



The majority of the EAOPs are based on the in situ electrogeneration of hydroxyl radical ( $\bullet\text{OH}$ ) mediators because they have greater standard reduction potentials than other reactive oxygen species, such as superoxide radical, ozone, hydrogen peroxide, or sulfate radical [63, 64]. However, it has been assumed that,

during water oxidation  $\bullet\text{OH}$  is formed (as shown in Eq. (1)) which participates in two additional reactions:  $\bullet\text{OH}$  oxidized to  $\text{O}_2$  (Eq. (2)) and contribute in dye mineralization (Eq. (3)) [65, 66].



However, the effectiveness of this procedure depends on the nature of the anode material because it determines the type of electrogenerated oxidants and their oxidation power [67].

### **II.1.5.2 Anodic materials**

Anodic materials with high oxygen evolution overpotential are generally preferred for electrochemical oxidation (EO) treatment, with boron-doped diamond (BDD) anodes being an excellent example [68-71]. BDD anodes outperform materials like platinum (Pt) and lead dioxide ( $\text{PbO}_2$ ) by producing greater quantities of reactive hydroxyl radicals ( $\bullet\text{OH}$ ). BDD possesses unique properties, including an exceptionally wide potential window, corrosion stability in highly aggressive environments, low adsorption on their inert surface, strong resistance to deactivation, and robust oxidation capacity. These characteristics have made BDD electrodes extensively studied and widely applied in wastewater treatment [72]. The BDD electrode has proven to be a good choice, especially in the treatment of textile wastewater [73-74].

Boron-Doped Diamond (BDD) anodes perform efficiently with sodium sulfate ( $\text{Na}_2\text{SO}_4$ ) as the supporting electrolyte, as it avoids producing harmful byproducts such as organic chlorinated compounds found in chloride-based media [75].

Nevertheless, the application of BDD for wastewater depuration is limited by its high acquisition cost. As a result, research into various anode materials has been conducted to uncover less expensive electrodes as viable alternatives for lowering initial investment and operating expenses. This is the case of dimensional stable anodes (DSA) [76-88], which have a significant contact between their surface (M) and  $\bullet\text{OH}$  radicals. DSAs are titanium anodes covered with a mixed

metal oxide, which composition includes elements such as iridium, ruthenium, platinum, rhodium, and tantalum [89].

The electro-catalytic behavior and activity of electrodes depend on the nature of the electrode material. Dimensionally stable anodes (DSAs), such as titanium dioxide ( $\text{TiO}_2$ ), ruthenium dioxide ( $\text{RuO}_2$ ), and iridium dioxide ( $\text{IrO}_2$ ), are widely used in the electrochemical treatment of dye-containing effluents due to their high chemical and mechanical stability, even under strong acid conditions and high current densities [90,91]. These electrodes provide excellent durability and performance, making them ideal for long-term applications in wastewater treatment [92]. Other electrodes, including graphite, Pt, lead dioxide ( $\text{PbO}_2$ ), tin oxide ( $\text{SnO}_2$ ), and BDD, are also used, though their stability and catalytic properties vary. Compared to conventional anodes, DSAs offer superior durability and electro-catalytic efficiency, particularly under harsh operating conditions [93-95].

Nowadays, researchers enhance titanium substrate anodes by doping them with noble metal oxides, such as  $\text{RuO}_2$  and  $\text{IrO}_2$ , to improve corrosion resistance and electrode longevity [96]. These materials belong to the category of active electrodes, meaning they participate in electrochemical reactions by forming intermediate species that promote pollutant degradation. Among them,  $\text{RuO}_2$  is particularly intriguing due to its superior electrocatalytic capabilities, while  $\text{IrO}_2$  offers greater stability and a longer service lifetime [97]. In contrast, non-active electrodes, such as BDD and  $\text{PbO}_2$ , do not actively participate in redox reactions but instead generate hydroxyl radicals ( $\bullet\text{OH}$ ) for indirect oxidation [98].

Electrochemical oxidation is an effective and clean technology for wastewater treatment due to its strong oxidation power and ability to degrade persistent organic pollutants [99,100]. Its efficiency depends on the choice of anode and cathode materials [101]. Studies suggest that commercial anodes like  $\text{Ti/IrO}_2$ ,  $\text{Ti/RuO}_2$ , and BDD are effective for color and COD removal in industrial textile wastewater [102]. In practical applications, stainless steel is an ideal cathode due to its durability, cost-effectiveness, and stability [103,104].

## **II.2 Portuguese legislation for wastewater treatment**

The discharge of industrial wastewater into water bodies and its reuse are regulated by directives and standards established under the framework of European Union legislation.

Adherence to maximum concentration thresholds for parameters such as Chemical Oxygen Demand (COD), and pH is essential.

In Portugal, according to the ministry of environment's Decree-Law No. 236/98, for the effluent to be discharged in the aquatic medium, COD levels must be maintained below 150 mgO<sub>2</sub> /L to prevent excessive oxygen depletion in aquatic ecosystems, while pH should fall within the specified range of 6.0 to 9.0 to prevent adverse effects on water quality and aquatic life. The color of the water is also a crucial factor to consider when assessing its quality and compliance with legislation, as it should not be visible in a 1:20 dilution.

By carefully monitoring and managing these parameters, industries can mitigate environmental impacts, uphold regulatory standards, and optimize the potential for wastewater reuse in a sustainable manner [105].

## **CHAPTER III**

# **MATERIALS AND METHODS**

The experimental approach of this study begins with preparing a synthetic solution that mimics the composition of textile wastewater as closely as possible. This solution allows for precise control over experimental conditions and facilitates the detailed exploration needed to optimize the electrolytic treatment, before applying them to real industrial effluent. By conducting preliminary experiments in a controlled environment, we seek to understand the behavior and interactions of experimental parameters that influence the treatment process. Each experiment was conducted separately, with only one parameter changed at a time. This systematic shuffling of conditions allows for a comprehensive understanding of how each factor contributes to overall performance.

### III.1.1 Methylene blue solution preparation

The methylene blue (MB), Fig.III.1, solution simulates an actual textile wastewater. This controlled preparation method allows for repeatable and accurate experiments, ensuring that solutions can be made consistently under identical conditions to yield reliable and precise results. In fact, this solution was prepared by dissolving 0.1 g of MB ( $C_{16}H_{18}ClN_3S \cdot xH_2O$ , Sigma Aldrich,  $\geq 98\%$  purity) in 1 L of distilled water, yielding a 100 ppm concentration.

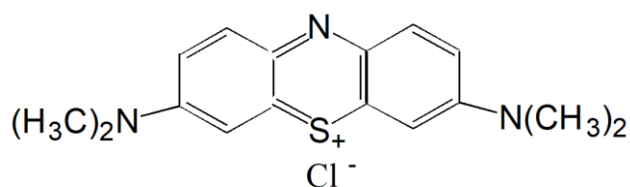


**Figure III.1:** Chemical formula of methylene blue.

An amount of approximately 7 g of sodium sulfate ( $Na_2SO_4$ , Sigma Aldrich,  $\geq 99\%$  purity) was added to the solution, acting as the supporting electrolyte which is essential for enhancing ionic conductivity, ensuring efficient current flow and stable electrochemical reactions. This helps maintain a consistent electric field and reduces voltage drops, which supports effective treatment. Sodium sulfate is chosen for its inert properties, preventing unwanted side reactions and providing a reliable ionic background for the process. An ultrasonic bath is used to mix the solution for 15 to 20 minutes, without applying heat. This prevents any changes to the solution and

keeps it stable for electrochemical treatment. This ensures that the methylene blue and  $\text{Na}_2\text{SO}_4$  dissolves evenly and is prepared properly for the experiments.

It should be noted that the maximum wavelength absorption of methylene blue was found to be equal to 663.5 nm with respect to peak number one, as shown in Fig.III.2.

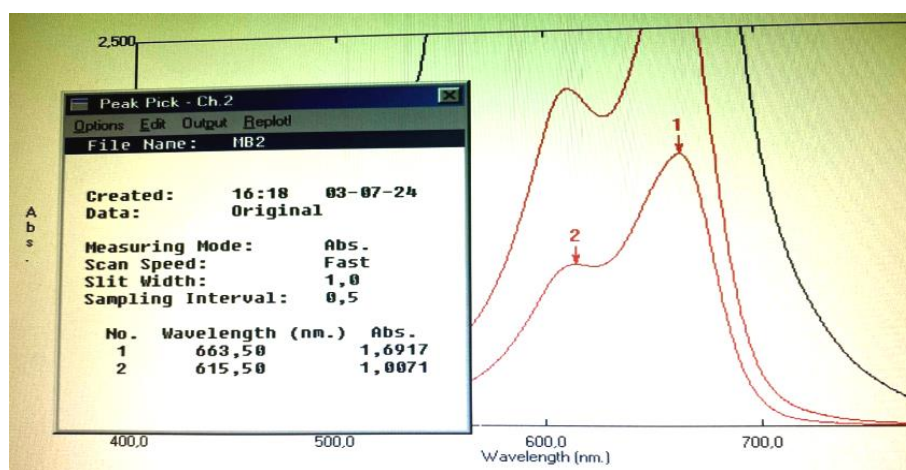


**Figure III.2:** UV-vis spectra of MB

### III.1.2 Electrochemical setup

The electrochemical oxidation (EO) process was conducted using a power supply (TTI EX752M MULTIMODE PSU 75V/150V 300W) connected to commercially available electrodes. Anodes: boron-doped diamond (BDD), titanium coated with ruthenium dioxide ( $\text{Ti/RuO}_2$ ) and titanium coated with iridium dioxide ( $\text{Ti/IrO}_2$ ). A stainless-steel cathode complemented the system to facilitate the electrochemical reactions necessary for the removal of color and reduction of chemical oxygen demand (COD) from the solution. To set up the system, the power supply was used to control the electrical current applied to the electrodes. The positive terminal (+) will be connected to the anode (BDD,  $\text{Ti/RuO}_2$ , or  $\text{Ti/IrO}_2$ ), while the negative terminal (-) will be linked to the stainless-steel cathode. This configuration ensures that the current flows appropriately through the solution, enabling the electrochemical reactions necessary for contaminant degradation Fig III.3. (a).

The experiments were conducted in a 200 mL beaker containing the prepared MB solution.

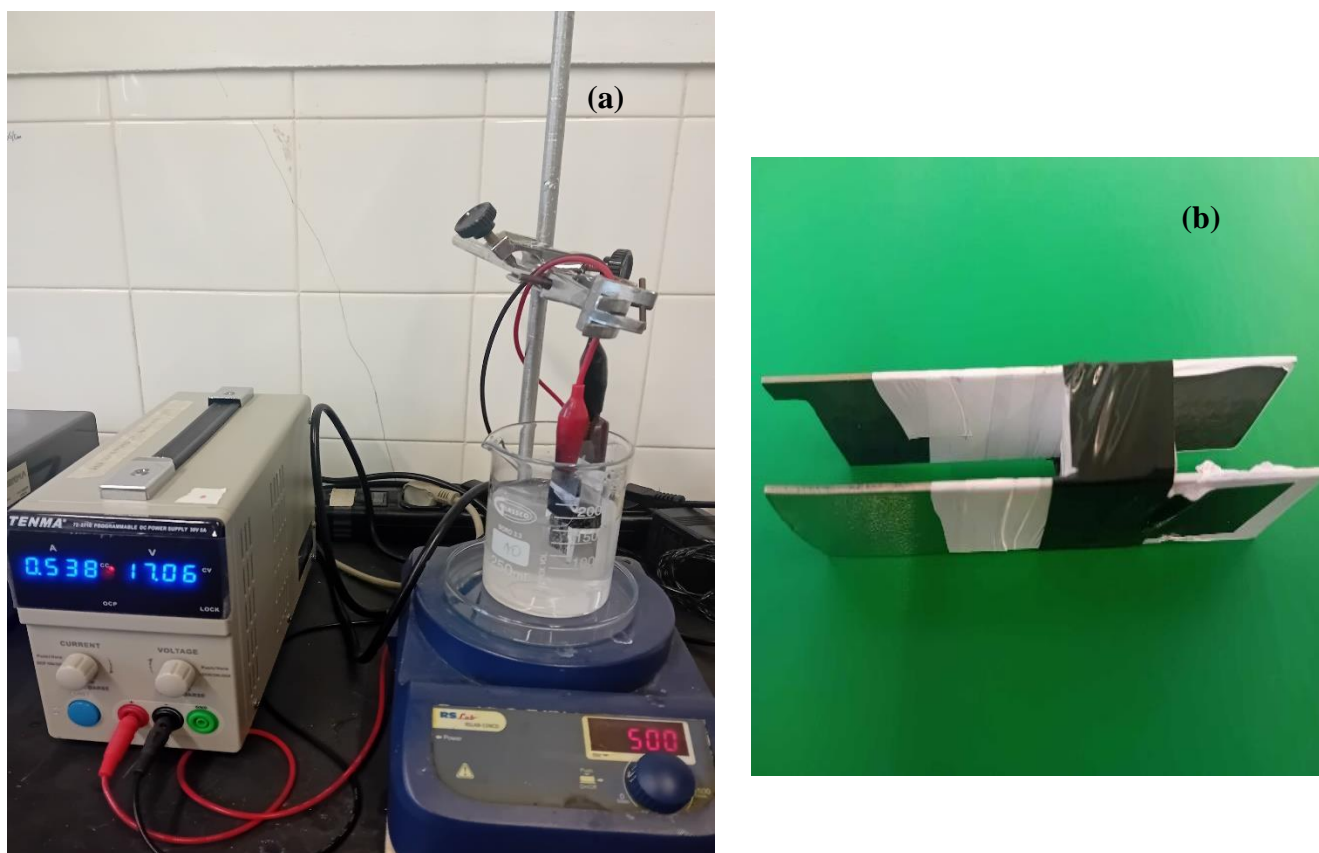


**Figure III.3:** Electrochemical setup (a) and electrodes with acrylic spacers covered with Teflon (b)

The beaker is equipped with a magnetic stirrer to maintain consistent mixing, distributing the solution evenly and ensuring effective contact between the solution and the electrode surfaces. The values tested were 250, 500 and 750 rpm. All electrodes used in the experiments had an exposed active surface area of  $4.5 \text{ cm}^2$  delimited with Teflon, submerged in the solution Fig.III.3 (b).

The electrode bottom was kept 5 cm above the magnetic stirrer to avoid direct interference from the magnetic field and ensure uniform mixing without disrupting the electrochemical reaction.

Electrodes were spaced at adjustable distances (0.5, 1 and 2 cm) using acrylic spacers to evaluate the impact of electrode positioning on the current distribution and overall process performance. The current intensity was carefully controlled and

set at 0.031, 0.06 and 0.12 A/cm<sup>2</sup> to investigate how different electrical energy inputs influence the generation of oxidizing agents and the subsequent breakdown of contaminants.

### **III.1.3 Treatment plan for monitoring the electrochemical process's efficiency**

Each experiment in the study lasted 360 minutes and was conducted in a controlled environment to systematically investigate the behavior and interactions of key experimental parameters influencing the electrolytic treatment process. Only one parameter was varied at a time, allowing for clear attribution of effects and comprehensive understanding. Initially, we tested current densities of 0.031 A/cm<sup>2</sup>, 0.06 A/cm<sup>2</sup>, and 0.12 A/cm<sup>2</sup> while keeping the initial concentration fixed at 100 ppm, the mixing rate at 500 rpm, and the inter-electrode distance at 1 cm. Next, we fixed the current density at 0.06 A/cm<sup>2</sup>, the concentration at 100 ppm, and the mixing rate at 500 rpm, and varied the inter-electrode distance to 0.5 cm and 2 cm. After that, with the current density maintained at 0.06 A/cm<sup>2</sup>, the concentration at 100 ppm, and the inter-electrode distance at 0.5 cm, we varied the mixing rate from 250 rpm to 750 rpm. Finally, we fixed the current density at 0.06 A/cm<sup>2</sup>, the inter-electrode distance at 0.5 cm, and the mixing rate at 250 rpm, and varied the initial concentration of methylene blue from 50 ppm to 200 ppm. This systematic shuffling of conditions enabled a comprehensive understanding of how each factor contributes to the overall performance, needed for the optimization of the electrolytic treatment process.

The pH and conductivity were determined prior to and following treatment. Chemical oxygen demand (COD) removal was evaluated using UV-Vis absorbance at a wavelength of 600nm, with readings acquired before and after the treatment.

Samples for color removal were periodically withdrawn at specific intervals (0, 5, 15, 30, 60, 90, 120, 180, 240, 300, and 360 min) for analysis. The withdrawn samples were diluted using distilled water before measuring their absorbance. The wavelength 663.5 nm was chosen for UV-Vis readings as it corresponds to the maximum absorbance of methylene blue, giving the highest peak. Measuring at this wavelength allows for accurate detection of dye concentration changes, enabling precise monitoring of the electrochemical treatment's effectiveness in degrading the contaminant and assessing the overall treatment performance. For color removal an

appropriate dilution was carried out to obtain measurable sample for absorbance recording.

Concerning samples collected from treatments using Ti/IrO<sub>2</sub> and Ti/RuO<sub>2</sub> anodes undergo a consistent 1:20 dilution. However, concerning the BDD anode, the dilution strategy varies based on the time of sampling and current intensity as shown in Table III.1.

**Table III.1:** Dilution plan for BDD anode.

Time	Current density		
	0.031 A/cm <sup>2</sup>	0.06 A/cm <sup>2</sup>	0.12 A/cm <sup>2</sup>
From 0 to 30min	1:20		
From 60 to 90 min	1:5		NO DILUTION
From 120 to 360 min	NO DILUTION		

## III.2 Analytical techniques

Tests for pH and conductivity were determined prior to and following treatment. Color and chemical oxygen demand (COD) removal were evaluated using UV-Vis absorbance.

### III.2.1 pH

The determination of pH of wastewater is crucial for assessing water quality and treatment efficacy. pH levels influence chemical reactions during treatment processes, and it is detected by measuring the concentration of hydrogen ions (H<sup>+</sup>) present in the water. It determines the acidity or alkalinity of a solution and is expressed on a scale from 0 to 14 [106]. In this study, the pH measurements were performed using multimeter WTW Laboratory pH Meter inoLab® Multi 9620 IDS SET C, Fig.II.4. Calibration was performed prior to each set of measurements using standard buffer solutions with pH values of 4.00, 7.00 and 10.00, ensuring accuracy and reliability of the readings. Regular calibration minimizes

instrumental drift, and guarantees the precision required for assessing treatment efficiency.

### III.2.2 Conductivity

Conductivity is a measurement of a substance's ability to conduct an electric current. In the context of water, conductivity is frequently used as an indicator of its impurity or the concentration of dissolved ions. The higher the conductivity, the more ions exist in the water.

A conductivity meter; conductometer, is the principal instrument used to measure conductivity. It comprises of two electrodes made of graphite or metal embedded in the water sample. An electric current is passed between the electrodes and the meter measures the resistance to the flow of this current. Conductivity is commonly measured in siemens per meter ( $\text{S}\cdot\text{cm}^{-1}$ ) or microsiemens per centimeter ( $\mu\text{S}\cdot\text{cm}^{-1}$ ) and millisiemens per centimeter ( $\text{mS}\cdot\text{cm}^{-1}$ ) [107]. The conductivity was measured using the same multimeter WTW Laboratory pH Meter inoLab® Multi 9620 IDS SET C, Fig III.4. Prior to measurements, the instrument was calibrated using a standard potassium chloride (KCl) solution with a known conductivity of 150  $\mu\text{S}/\text{cm}$ , 1170  $\mu\text{S}/\text{cm}$  and 10  $\text{mS}/\text{cm}$ , thereby enhancing the reproducibility and validity of the conductivity data collected during the treatment process.



**Figure III.4:** Multimeter used for pH and conductivity measurements.

### III.2.3 Absorbance (UV-Vis)

The UV-Vis absorbance analysis, known as Ultraviolet/visible (UV-Vis) spectroscopy, is a typical analytical technique for determining the composition and concentration of compounds in a solution by measuring the absorbance of ultraviolet (UV) or visible light [108]. The preparation methodology for each solution involved a specific dilution protocol, or the absence thereof, contingent upon the initial concentration requirements.

In this study, a UV VIS spectrophotometer, Single Beam, VWR UV-1600PC was used for the absorbance measurements, Fig. III.5.,



**Figure III.5:** UV-Vis spectrophotometer.

Color removal was measured in % removal using efficiency formula:

$$\text{Color removal (\%)} = \frac{A_0 - A_t}{A_0} \times 100 \quad (\text{Eq (4)})$$

Where:

- $A_0$  is the initial absorbance (before treatment)
- $A_t$  is the absorbance after treatment.

This formula helps determine the efficiency of color removal in water or wastewater treatment processes by measuring the reduction in absorbance, which correlates to the concentration of color-causing substances [109].

### III.2.4 Chemical oxygen demand (COD)

The COD is a measure of the overall quantity of oxygen utilized by chemical reactions that oxidize pollutants in water. This covers the oxidation of organic and inorganic compounds found in the water sample. High COD levels indicate a greater amount of oxidizable pollutants in water, which can lead to oxygen depletion when these pollutants are discharged into natural water bodies. The steps of carrying out the COD analysis were as follows:

- Reagents: potassium dichromate ( $K_2Cr_2O_7$ ) solution as the oxidizing agent and sulfuric acid ( $H_2SO_4$ ) solution as a catalyst.
- Digestion: in a COD glass vial containing already the potassium dichromate and sulfuric acid solutions, an amount of 2.5mL of wastewater sample is added. To ensure complete oxidation of the organic components, the mixture is heated at  $150^\circ C$  for 120 min.
- Cooling: after digesting, the vial is let to cool to room temperature for 120 min.
- Measurement: a spectrophotometer was used to measure the absorbance of samples at 600 nm. The absorbance is directly proportional to the number of oxidized organic molecules in the sample.
- Calibration: series of standard solutions containing known concentrations of a reference substance such as potassium hydrogen phthalate, were measured at 600 nm. Then, a calibration curve was established to correlate absorbance with concentration.
- Calculation: using the calibration curve, the concentration of COD in the wastewater sample was calculated through its absorbance value. The result is expressed in milligrams of oxygen consumed per liter of sample ( $mgO_2/L$  or ppm) [110].

COD removal was measured in % using efficiency formula:

$$COD\ removal\ (\%) = \frac{COD_i - COD_f}{COD_i} \times 100 \quad (Eq\ 5))$$

Where  $COD_i$  is initial COD and  $COD_f$  is final COD.

The calibration curve for COD is  $Abs=0.000305 \text{ COD} + 0.005050$ .

These calculations provide essential insights into the effectiveness of the electrochemical treatment by quantifying the extent of color and COD removal, which indicate the process's capability to degrade and remove contaminants [111].

### III.3 Industrial parameters

Calculating key performance indicators such as current efficiency and energy consumption, is necessary since these calculations are essential for analyzing and quantifying the effectiveness of the electrochemical treatment.

#### III.3.1 Energy consumption

Energy consumption was calculated using this formula:

$$\text{Energy consumption (kWh/gCOD)} = \frac{U \times I \times t}{1000 \times \Delta\text{COD} \times V} \quad (\text{Eq (6)})$$

**U** = Cell voltage (V)

**I** = Current (A)

**t** = Time (s)

**ΔCOD** = COD removed

**V** = Volume of treated solution (L)

**1000** = Conversion from watt-seconds (Joules) to kilowatt-hours

Energy consumption measures the electrical energy used during the electrochemical treatment. Calculating it helps determine the efficiency and cost-effectiveness of the process, ensuring it is suitable for practical and sustainable use [112].

#### III.3.2 Current efficiency

The current efficiency can then be determined from  $\Delta\text{COD}$  (in  $\text{g dm}^{-3}$ ) using the efficiency formula:

$$\text{Current efficiency(\%)} = \frac{(\Delta\text{COD})FVs}{8It} \times 100 \quad (\text{Eq (7)})$$

F: Faraday constant =  $96,487 \text{ C mol}^{-1}$

Vs: Solution volume (L)

I: Applied current (A)

8: Oxygen equivalent mass

t: electrolysis time (s)

Current efficiency is the ratio of the actual amount of desired electrochemical reaction products to the theoretical amount expected based on the total charge passed through the system. It indicates how effectively the electric current is utilized, with losses typically caused by side reactions or inefficiencies in the process [112].

Together, these metrics allow for a comprehensive assessment of the treatment process, validating the optimized conditions for maximum contaminant removal and efficient energy use in real-world applications.

#### **IV. Statistical method**

Each experiment was conducted in triplicate (n=3) to enable the statistical characterization of the outcomes. Specifically, the mean of the results was calculated to establish their central tendency. The mean representing the average value, was computed using the formula:

$$x = \frac{\sum_{i=1}^n x_i}{n}$$

where  $x_i$  represents each individual measurement and  $n$  is the number of measurements.

While the standard deviation was determined to quantify the spread of individual measurements around this central value. The standard deviation (s) measures the dispersion of data points around the mean and was calculated as:

$$S = \sqrt{\frac{\sum_{i=1}^n (x_i - x)^2}{n-1}}$$

This method of triplicate repetition afforded a sufficient basis for understanding the representative result and its associated dispersion, adhering to established principles of experimental design and data analysis [113].

## **CHAPTER IV**

# **RESULTS AND DISCUSSION**

This chapter provides a comprehensive analysis of the results using different types of anodes, focusing on the impact of key parameters such as current density, inter-electrode distance, and mixing rate on color and chemical oxygen demand COD removal efficiencies.

## **IV.1 Characterization of the synthetic effluent**

The synthetic effluent, a methylene blue solution, exhibited an average pH of  $6.65 \pm 0.04$  (95% CI: [6.61, 6.69]), indicating a slightly acidic to neutral nature, which is typical for such dye solutions. At 663.5 nm, the 100 ppm methylene blue solution had an initial absorbance averaging  $0.97 \pm 0.01$  (95% CI: [0.96, 0.98]). The Chemical Oxygen Demand (COD) was measured at  $280.07 \pm 0.01$  mgO<sub>2</sub>/L (95% CI: [280.06, 280.08]), reflecting a moderate yet significant organic load, characteristic of industrial dye wastewater. Additionally, the electrical conductivity averaged  $8.16 \pm 0.03$  mS/cm (95% CI: [8.13, 8.19]), suggesting a moderate concentration of dissolved ions crucial for enabling electrochemical reactions. This effluent was precisely prepared at a concentration of 100 ppm, corresponding to 1 gram of methylene blue dissolved in 1 liter of distilled water. These comprehensive values provide critical insight into the initial physicochemical characteristics of the effluent's composition and its potential environmental impact, guiding the optimization of the treatment process.

## **IV.2 Effect of the current density on color and COD removal**

Color removal is a vital indicator of the efficiency of electrochemical treatment processes. The experiments were designed to evaluate the impact of varying current densities 0.031, 0.06 and 0.12 A/cm<sup>2</sup> on the removal of color from wastewater. A mixing speed of 500 rpm and an inter-electrode distance of 1 cm were maintained throughout the experiments to ensure uniform distribution of reactive species and optimal interaction between the electrodes. The initial concentration of methylene blue in the stock solution was set at 100 ppm. The goal was to assess how different current densities influence color and COD removal efficiency, demonstrating the potential of electrochemical methods for wastewater treatment, providing insights into the degradation efficiency over time.

### **IV.2.1 Effect of the current density on color removal**

At 0.031 A/cm<sup>2</sup> the BDD (Boron-Doped Diamond) anode demonstrated exceptional performance, achieving nearly 70% color removal within the first 100 minutes and maintaining this efficiency throughout the experiment. This highlights its strong ability to generate reactive oxygen species, even at low current densities, leading to rapid and effective dye degradation. Increasing the current density to 0.06 A/cm<sup>2</sup> further enhanced BDD's efficiency, achieving 80%

color removal within 100 minutes, reinforcing its superior oxidative capabilities. At 0.12 A/cm<sup>2</sup>, BDD continued to outperform the other electrodes, reaching 100% color removal in 100 minutes, confirming that higher current densities further improve its already exceptional performance, Fig IV.1 (a).

The Ti/IrO<sub>2</sub> (Titanium-Iridium Dioxide) anode showed moderate efficiency, with performance improving as current density increased. At 0.031 A/cm<sup>2</sup>, it achieved 35% color removal by the end of the 360-minute treatment, indicating limited reactive species generation. When the current density was increased to 0.06 A/cm<sup>2</sup>, its performance improved, reaching 54% color removal by the end of the experiment, demonstrating enhanced oxidation efficiency at higher densities. At 0.12 A/cm<sup>2</sup>, the Ti/IrO<sub>2</sub> anode exhibited 73 % color removal, showing a substantial improvement. This suggests that higher current densities significantly enhance its oxidative capabilities, although it remains less effective than BDD, Fig IV.1 (b).

The Ti/RuO<sub>2</sub> (Titanium-Ruthenium Dioxide) anode exhibited the lowest efficiency among the three electrodes. At 0.031 A/cm<sup>2</sup>, it achieved 25% color removal by the end of the experiment, indicating weak oxidation power at low current density. When the current density was increased to 0.06 A/cm<sup>2</sup>, the Ti/RuO<sub>2</sub> anode showed a slight improvement, reaching 35% color removal, but it remained the least effective electrode. At 0.12 A/cm<sup>2</sup>, its efficiency improved further, reaching 56% color removal. However, even at its best, Ti/RuO<sub>2</sub> remained significantly less effective than both BDD and Ti/IrO<sub>2</sub>, highlighting its weaker oxidative potential, Fig IV.1 (c).

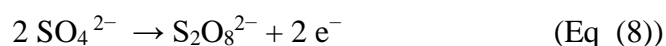
Higher current densities enhance color removal for all tested anodes, with BDD consistently achieving the fastest and most complete removal. Ti/IrO<sub>2</sub> showed substantial improvement at higher currents, while Ti/RuO<sub>2</sub> exhibited moderate gains, emphasizing the critical role of current density in optimizing electrochemical dye removal processes.

BDD anodes are considered non-active electrodes due to their extremely high oxygen evolution potential. This property, combined with their chemical inertness, promotes the generation of highly reactive hydroxyl radicals ( $\cdot\text{OH}$ ) from the oxidation of water (eq (1)). These ( $\cdot\text{OH}$ ) radicals are exceptionally potent, non-selective oxidants that readily attack a broad spectrum of organic pollutants like methylene blue, leading to their degradation in the bulk solution through an indirect oxidation mechanism. This leads to the complete mineralization of the dye into CO<sub>2</sub>, water, and inorganic ions, making BDD anodes highly effective for broad-spectrum pollutant degradation [114].

Unlike BDD, Ti/IrO<sub>2</sub> and Ti/RuO<sub>2</sub> are active electrodes because their lower oxygen evolution potential allows their surface metal ions to achieve higher oxidation states when an anodic potential is applied. These more reactive metal oxides serve as direct active sites, for example, iridium in Ti/IrO<sub>2</sub> might transition from Ir(IV) to Ir(V) or Ir(VI) at the surface, initiating the degradation of methylene blue through electron transfer. Additionally, these active sites can facilitate the formation of adsorbed oxygen species or higher metal oxides which then react with the organic pollutant. This direct oxidation mechanism forms various intermediate species, which are subsequently oxidized until complete mineralization is achieved, turning the complex dye into simple inorganic compounds such as CO<sub>2</sub> and water [115].

Sodium sulfate was added to the wastewater as an electrolyte to enhance ionic conductivity. This increase in ions facilitates efficient current flow, ensuring a consistent electric field throughout the electrochemical cell. By reducing ohmic resistance and voltage drops, Na<sub>2</sub>SO<sub>4</sub> ensures stable electrochemical reactions and supports effective treatment without significant energy loss.

In the presence of sulfate ions (SO<sub>4</sub><sup>2-</sup>), particularly at high anodic potentials, persulfate ions (S<sub>2</sub>O<sub>8</sub><sup>2-</sup>), a strong oxidant, can be formed through the following reaction:



Persulfate is a powerful oxidizing agent that can directly react with organic pollutants or be activated to form sulfate radicals (SO<sub>4</sub>·<sup>-</sup>), another highly reactive species:



These radicals significantly contribute to the degradation of methylene blue by initiating chain reactions and oxidizing the dye molecules, thereby enhancing the overall treatment efficiency [116].

In a related study conducted by Ogutveren et al., similar patterns were observed, where an experiment was conducted to study the influence of current density (2, 4 and 6 mA/cm<sup>2</sup>) on the removal of RR-120 dye from drinking water using electrochemical oxidation process. The results obtained showed that the removal of dye from the synthetic water samples increases with the increase of the applied current density. Aljaberi and al., has also found that the removal efficiency, after 8 minutes of treatment, has increased from 80% to 88% and 96% as the current density increased from 2 to 4, and 6 mA/cm<sup>2</sup>, respectively. This is explained by the fact that

increasing the current density increases the dissolving rate of aluminium ions from the anode, which enhances the dye removal. However, increasing the applied current density results in an increase in power consumption, thus current density of  $4 \text{ mA}\cdot\text{cm}^2$  will be used to carry out the rest of experiments [117, 118].

#### **IV.2.2 Effect of current density on chemical oxygen demand (COD)**

Chemical Oxygen Demand (COD) is a critical parameter used to evaluate the organic pollution level in wastewater. Measurements of COD were taken at the beginning and after 360 minutes of electrochemical treatment to determine the extent of its reduction under varying current intensities, using Equation 6 (Eq (6)) and the calibration curve.

At  $0.031 \text{ A}/\text{cm}^2$ , the BDD anode exhibited the highest COD removal efficiency among all electrodes, achieving 20% removal achieving  $229.34 \text{ mgO}_2/\text{L}$ . However, COD reduction remained relatively low at this current intensity due to the limited production of reactive oxygen species. Despite this, BDD's superior oxidative capabilities allowed it to outperform the other anodes. Increasing the current intensity to  $0.06 \text{ A}/\text{cm}^2$  significantly improved COD removal reaching 30% efficiency having a final COD of  $198.2 \text{ mgO}_2/\text{L}$ , highlighting its enhanced ability to generate reactive oxygen species essential for organic pollutant degradation. At  $0.12 \text{ A}/\text{cm}^2$ , BDD achieved the highest COD removal, reaching 41% with a final COD of  $167.05 \text{ mgO}_2/\text{L}$ , demonstrating that higher current intensities further enhance its electrochemical oxidation efficiency, Fig IV.1 (d).

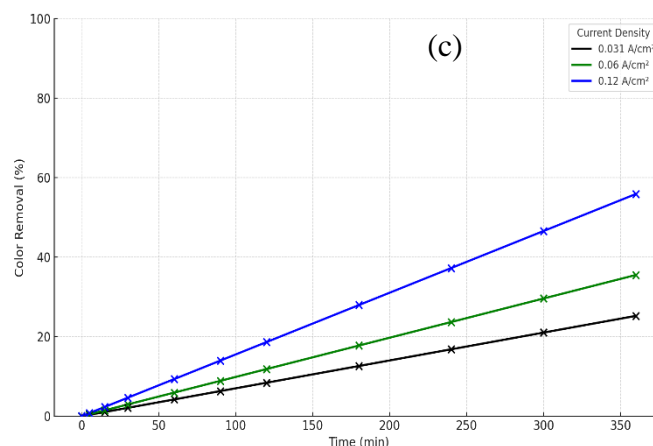
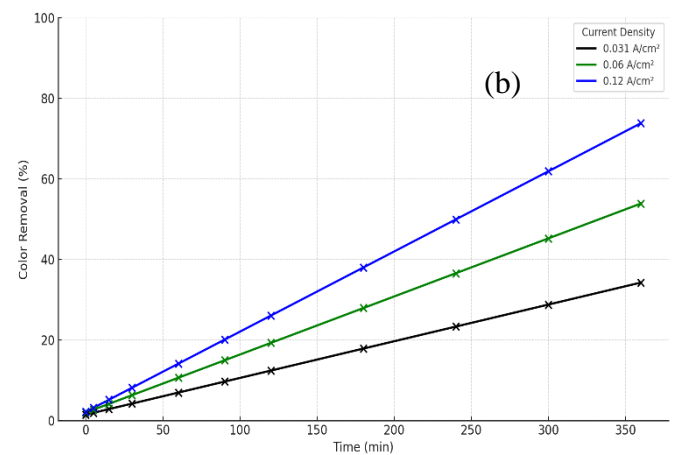
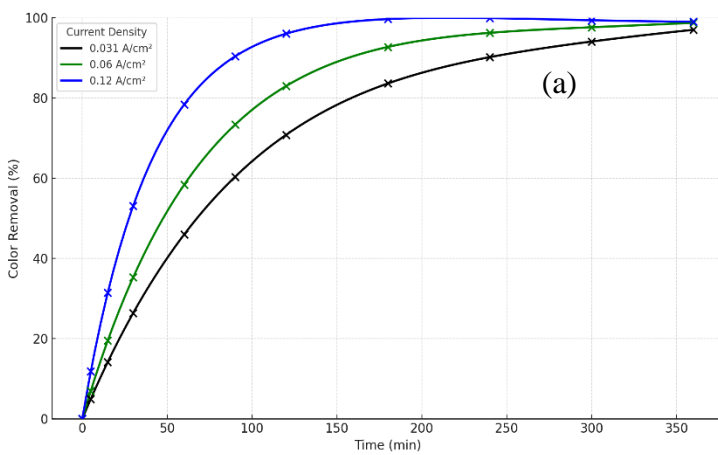
The  $\text{Ti}/\text{IrO}_2$  anode showed relatively low COD removal efficiency, particularly at lower current densities. At  $0.031 \text{ A}/\text{cm}^2$ , COD removal was at 9.1%,  $262.13 \text{ mgO}_2/\text{L}$ , indicating limited oxidative potential under these conditions. As the current density increased to  $0.06 \text{ A}/\text{cm}^2$ ,  $\text{Ti}/\text{IrO}_2$  showed only a slight improvement, achieving 16.56% COD removal reaching  $237.54 \text{ mgO}_2/\text{L}$ , significantly lower than BDD. At  $0.12 \text{ A}/\text{cm}^2$ , its performance improved more noticeably, reaching 22.64% COD removal reaching  $222.79 \text{ mgO}_2/\text{L}$ . This suggests that  $\text{Ti}/\text{IrO}_2$  benefits from higher current densities, but it remains significantly less effective than BDD in breaking down organic pollutants, Fig IV.1 (d).

The  $\text{Ti}/\text{RuO}_2$  anode demonstrated the lowest COD removal efficiency among the three electrodes. At  $0.031 \text{ A}/\text{cm}^2$ , COD removal was 6.02%, reaching  $273.61 \text{ mgO}_2/\text{L}$ , due to limited reactive species generation. At  $0.06 \text{ A}/\text{cm}^2$ , COD removal slightly improved, reaching only

11.42% with a final value of COD of 250 mgO<sub>2</sub>/L, indicating weak oxidation capabilities even at moderate current densities. At 0.12 A/cm<sup>2</sup>, Ti/RuO<sub>2</sub> showed its highest performance, achieving 15.58% COD removal reaching at the end 222.79 mgO<sub>2</sub>/L, yet it remained the least effective electrode in COD degradation, Fig IV.1 (d).

Increasing current density enhances COD removal efficiency for all anodes tested. BDD consistently outperformed Ti/RuO<sub>2</sub> and Ti/IrO<sub>2</sub>, showing the highest COD removal across all current settings due to its superior ability to generate reactive oxygen species. While all anodes benefited from higher current density, BDD demonstrated the most effective and reliable performance, making it the optimal choice for achieving significant COD reduction, with the Ti/RuO<sub>2</sub> anode exhibiting significantly lower oxidative power compared to Ti/IrO<sub>2</sub> as depicted in, Fig IV.1 (d).

In a separate study conducted by Jiachao Yao et al., similar tendencies were reported, where increasing current intensity led to improved COD removal efficiency as shows the figure below. It has increased from 78.4% to 95.3% as current density increased from 5.0 to 12.5 mA/cm<sup>2</sup>, though increasing current density was conducive to pollutant removal, the energy consumption would increase obviously. Current density of 10 mA/cm<sup>2</sup> was thus selected as the optimal one [119].



<<

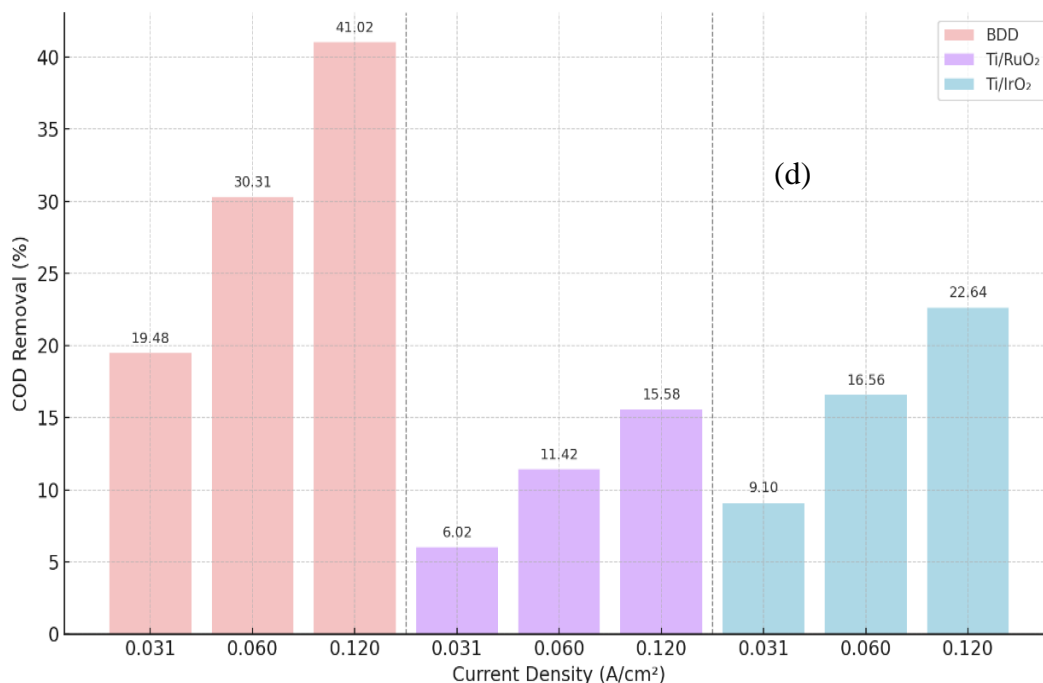


**Figure IV.1:** Effect of current density on color removal and on chemical oxygen demand (COD). (a): Effect of current density on color removal using BDD anode, (b): Effect of current density on color removal using Ti/IrO<sub>2</sub> anode, (c): Effect of current density on color removal using Ti/RuO<sub>2</sub>, (d): Effect of current density on chemical oxygen demand (COD) for all the anodes (d). The COD obtained for all electrodes is at 360 minutes.

At lower current densities, all anodes showed mild electrochemical activity, with minimal changes in pH and conductivity. The pH remained near neutral, and only slight variations in conductivity were observed, indicating limited ion generation or consumption. As current density increased, the electrochemical reactions became more intense, especially with the BDD anode, which promoted a strong alkaline shift and a marked increase in conductivity due to its strong oxidative power that promotes extensive breakdown of compounds, leading to high ion release and a pronounced shift toward alkaline conditions. In contrast, Ti/IrO<sub>2</sub> and Ti/RuO<sub>2</sub> showed more moderate responses, with less pronounced changes in pH and conductivity, as depicted in Table IV.1.

**Table IV.1:** pH and conductivity evolution for the electrodes at different current densities. The conductivity and pH obtained for all electrodes is at 360 minutes.

<b>Current density</b>	<b>Parameters</b>	<b>BDD</b>	<b>Ti/IrO<sub>2</sub></b>	<b>Ti/RuO<sub>2</sub></b>
<b>0.031 A/cm<sup>2</sup></b>	<b>pH</b>	7.6	7.7	7.6
	<b>Conductivity (mS/cm)</b>	8.6	8.9	8.9
<b>0.06 A/cm<sup>2</sup></b>	<b>pH</b>	10.1	7.2	7.4
	<b>Conductivity (mS/cm)</b>	8.9	8.45	8.8
<b>0.12 A/cm<sup>2</sup></b>	<b>pH</b>	11.6	7.1	7.3
	<b>Conductivity (mS/cm)</b>	10.5	9.5	9.3

A current density of 0.06 A/cm<sup>2</sup> and the BDD anode were selected for further experimentation, with the system operating at a rotation speed of 500 rpm. This configuration, identified by its low energy consumption (EC) and high current efficiency (CE), offers an ideal approach for analyzing electrochemical treatment processes.

This condition offers a highly efficient energy conversion, where the input electrical work is predominantly directed towards the target reactions, minimizing energy losses. This led to effective color and COD removal. In contrast, using other anodes resulted in higher energy consumption coupled with lower current efficiency, Fig IV.2, indicating an inefficient process which is characterized by substantial energy dissipation, reduced overall system productivity, and escalated operational costs due to the ineffective utilization of supplied energy.

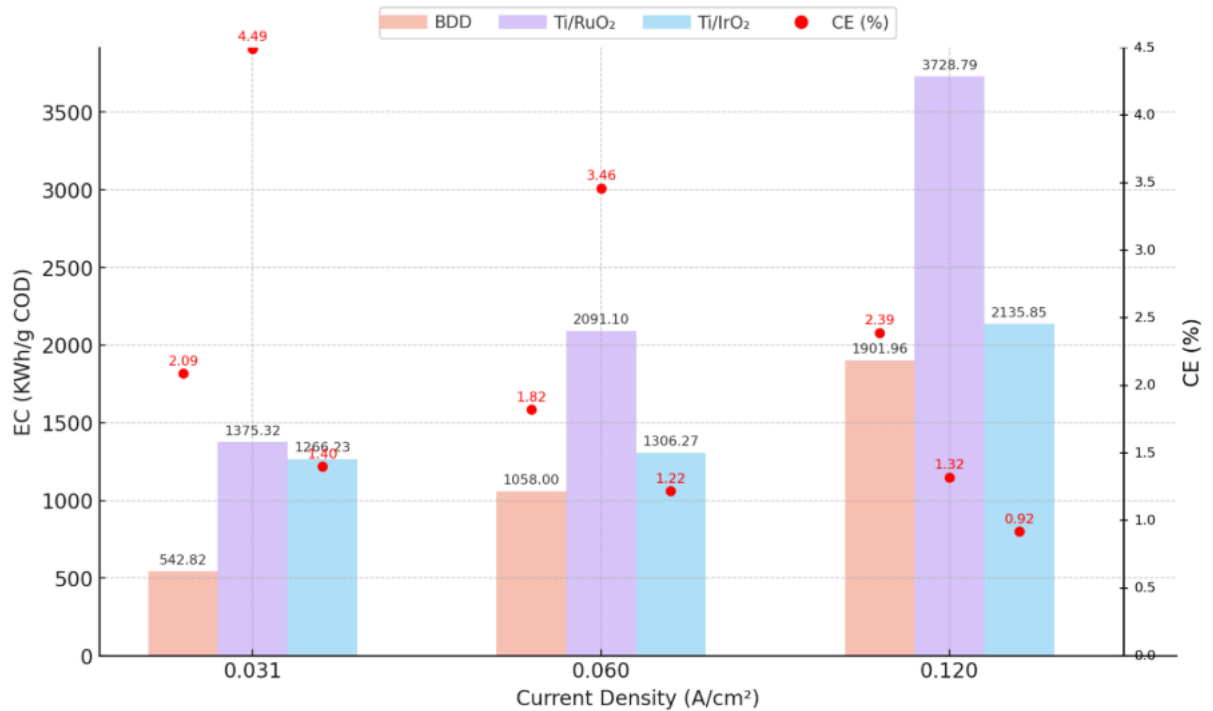


**Figure IV.2:** The energy consumption (EC) and the current efficiency (CE) for all the electrodes at different current densities. Bars correspond to EC and dots correspond to CE.

### IV.3 Effect of inter-electrode distance on color and COD removal

A parameter of interest was the distance between the electrodes and its influence on COD reduction and color removal. The tests were conducted with BDD and a stainless steel cathode, using inter-electrode distances of 0.5 cm and 2 cm, while maintaining a continuous mixing rate of 500 rpm for a total of 360 min of operation. The initial concentration of methylene blue in the stock solution was set at 100 ppm. The impact of the electrode spacing on both COD reduction and color removal efficiency was observed.

#### IV.3.1 Effect of inter-electrode distance on color removal

Both inter-electrode distances (0.5cm and 2cm) achieved complete color removal  $100\% \pm 0.00$ . The decolorization process exhibited excellent precision. Although the final removal efficiency was the same, the shorter distance of 0.5 cm led to faster decolorization, achieving near-complete color removal more quickly. Whereas at 2 cm, complete color removal took longer suggesting that a wider spacing slows the kinetics of the discoloration reaction. Thus, while the inter-

electrode distance does not affect the final color removal outcome, it clearly influences the rate at which it is achieved, FIGURE IV. 3 (a).

### IV.3.2 Effect of inter-electrode distance on COD removal

In contrast to color removal, COD removal was strongly affected by the inter-electrode distance with an initial COD value of 283.44 mgO<sub>2</sub>/L. At 0.5 cm, the system achieved 35.77 (±0.56), 95% CI [35.6, 35.9] reaching 185.08 mgO<sub>2</sub>/L, while at 2 cm, COD removal dropped significantly to 15.02 (±0.49), 95% CI [14.9, 15.1] reaching 242.46 mgO<sub>2</sub>/L, Fig IV.3 (b). Although both setups showed acceptable reproducibility, the performance at 0.5 cm was clearly superior. The lower efficiency observed when the inter-electrode distance is at 2 cm is likely due to a weakened electric field and limited generation of hydroxyl radicals, which are essential for the mineralization of organic compounds. These findings suggest that while extending the inter-electrode distance does not compromise decolorization, it substantially hinders the deeper oxidation required for effective COD reduction.

These findings highlight the importance of electrode spacing in optimizing electrochemical wastewater treatment processes, emphasizing that shorter distances improve both the rate of COD reduction and the speed of color removal.

Results showed that a shorter distance of 0.5 cm between the electrodes significantly enhanced the performance of the process. In contrast, an increased distance negatively impacts the efficiency of organic degradation. This decrease in performance is attributed to two main factors: a weakened electric field and reduced generation of reactive oxygen species at greater distances, as well as an increase in ohmic resistance  $R(\Omega)$ .

$$R(\Omega) = \frac{l}{\kappa \cdot A} \quad (\text{Eq (8)})$$

Where:

- $l$ : Inter-electrode distance (cm).
- $\kappa$ : Conductivity of the electrolyte (S/cm).
- $A$ : Cross-sectional area between the electrodes (cm<sup>2</sup>).

Ohmic resistance is the electrical resistance in the electrolyte that can impede current flow.

Accordingly, the resistance of the system increases proportionally with the inter-electrode distance (l), leading to higher power losses. The elevated ohmic resistance at larger distances hinders the flow of ions in the electrolyte, further reducing the system's efficiency and COD reduction capability [120].

The table shows the calculated ohmic resistance values for the two inter-electrode distances 0.5 cm and 2 cm, using a 0.05 M Na<sub>2</sub>SO<sub>4</sub> electrolyte prepared by dissolving exactly 7.102 g in 1 L of water. The electrolyte's conductivity at 25 °C is 0.0555 S/cm and the exposed electrode surface area is 4.5 cm<sup>2</sup>.

**Table IV.2:** calculated Ohmic resistance for the different inter-electrode distances.

<b>Inter-electrode distance</b>	<b>Ohmic resistance</b>
<b>0.5 cm</b>	2 Ω
<b>2cm</b>	8.01 Ω

Current density reduction with the increase of electrode distance was also observed by Phan et al., [121], and further mentioned by Thella et al. [122] as a consequence of resistance increase. This led to a decrease in electrostatic attraction, causing slower movement of the generated ions [123], and resulting in lower removal efficiency of pollutants, as noted by Fekete et al., this included a decrease in COD removal efficiency.

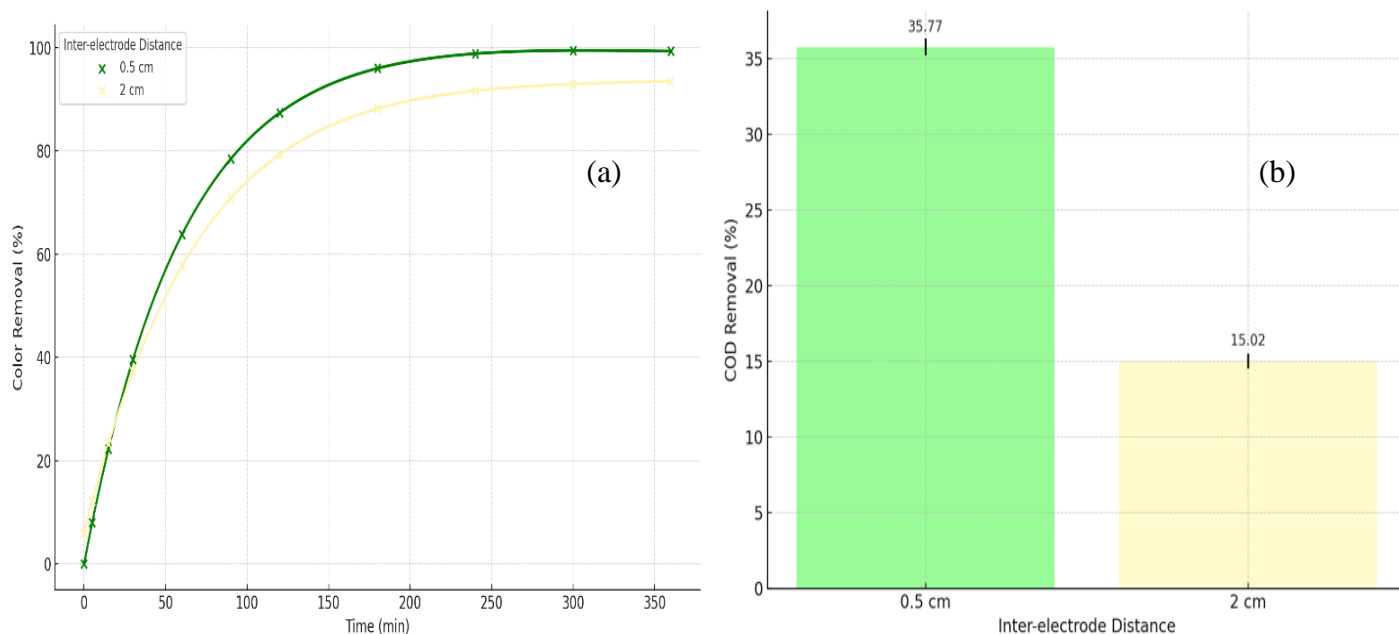


**Figure IV.3:** Effect of different inter-electrode distance on color and COD removal.

(a): Effect of different inter-electrode distance on color removal. (b): Effect of different inter-electrode distance on COD removal. The COD obtained is at 360 minutes.

An inter-electrode distance of 0.5 cm was selected for further experimentation, as it offered an optimal balance between conductivity and mass transfer. Combined with a current density of  $0.06 \text{ A/cm}^2$  and the use of BDD as the anode, this configuration provided efficient removal of both color and COD. This condition enables efficient energy conversion with minimal losses, with its low energy consumption (EC) and high current efficiency (CE), as shown in Fig IV.4, whereas an inter-electrode distance of 2cm exhibited high energy consumption and low current efficiency, reflecting poor energy utilization and increased operational costs.

This setup served as the reference configuration for assessing the effect of other experimental variables on treatment efficiency.

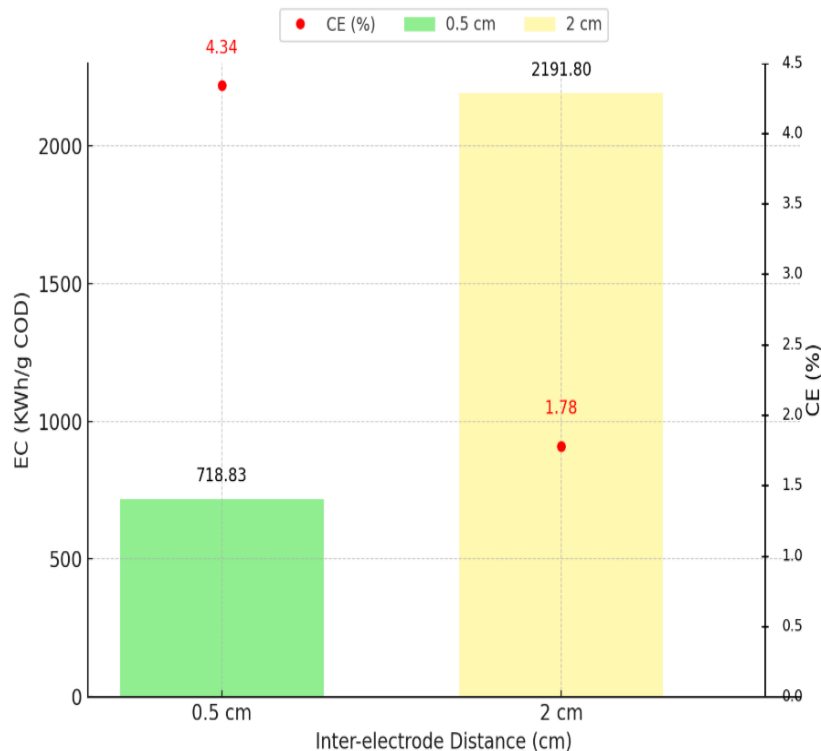


**Figure IV.4:** The energy consumption (EC) and current efficiency (CE) at different inter-electrode distances. Bars correspond to EC and dots correspond to CE.

#### IV.4 Effect of the mixing rate on color and COD removal

A current density of  $0.06 \text{ A/cm}^2$  and the BDD anode were selected for further experimentation due to their superior performance in color and COD removal. The initial concentration of methylene blue in the stock solution was set at 100 ppm. The system operated at a constant current intensity of  $0.06 \text{ A/cm}^2$  with varying mixing speeds to evaluate the influence of agitation on the electrochemical treatment efficiency. Tests were conducted using a stainless steel cathode and maintaining an inter-electrode distance of 0.5 cm for all experiments. Mixing speeds of 250 rpm and 750 rpm were applied over a 360-minute operation period to assess their effect on color and COD removal.

##### IV.4.1 Effect of the mixing rate on color removal

At an inter-electrode distance of 0.5 cm, color removal efficiency was assessed over 360 minutes at two stirring speeds: 250 rpm and 750 rpm. A faster initial rate of color removal was observed at 750 rpm, reaching approximately 88% by 90 minutes, whereas the 250 rpm setup reached around 81% in the same time frame. Subsequently, both systems continued to improve in efficiency, with the 250 rpm condition showing a more stable progression and achieving

complete color removal (100%) by 300 minutes. Color removal at 750 rpm, while initially faster, saw its process plateau and reach a steady state with only marginal improvements observed in the later stages, eventually also achieving 100% removal. These results indicate that while higher stirring speeds may enhance the early stages of color removal, moderate agitation at 250 rpm offers greater stability and ultimately achieves full color removal more rapidly over time and lead to more sustained and effective color removal.

Notably, the results at 250 rpm were optimal, Fig IV.5 (a), indicating a balance between mixing intensity and mass transfer efficiency, ensuring uniform distribution of reactants, and preventing concentration polarization at the electrode surface, thereby influencing the overall oxidation yield and the degradation of the existing pollutants.

#### **IV.4.2 Effect of the mixing rate on COD**

COD removal was notably higher at 250 rpm, achieving  $68.8 \pm 0.67$  (95% CI: [68.7, 68.9]) reaching 171.16 mgO<sub>2</sub>/L at the end, compared to 750 rpm at  $33.34 \pm 0.33$  (95% CI: [33.27, 33.41]) that was 342.39 mgO<sub>2</sub>/L, Fig IV.5 (b). Both exhibited excellent reproducibility. This disparity in performance highlights the critical role of mixing dynamics in electrochemical oxidation. Moderate stirring at 250 rpm ensures superior mass transfer of pollutants to the electrode surface and promotes consistent reaction with generated reactive oxygen species (ROS). In contrast, high agitation (750 rpm) leads to excessive turbulence that reduces the residence time of reactive species and pollutants at the electrode surface, thereby limiting degradation kinetics.

Mixing plays a crucial role in influencing ohmic resistance, which impacts electrochemical efficiency. At higher speeds, excessive turbulence can reduce the contact time between reactive species and pollutants, leading to localized variations in the electric field and increased resistance, ultimately decreasing treatment efficiency. Additionally, excessive turbulence can disrupt mass transfer, reducing the efficient movement of reactive species to pollutant sites [124].

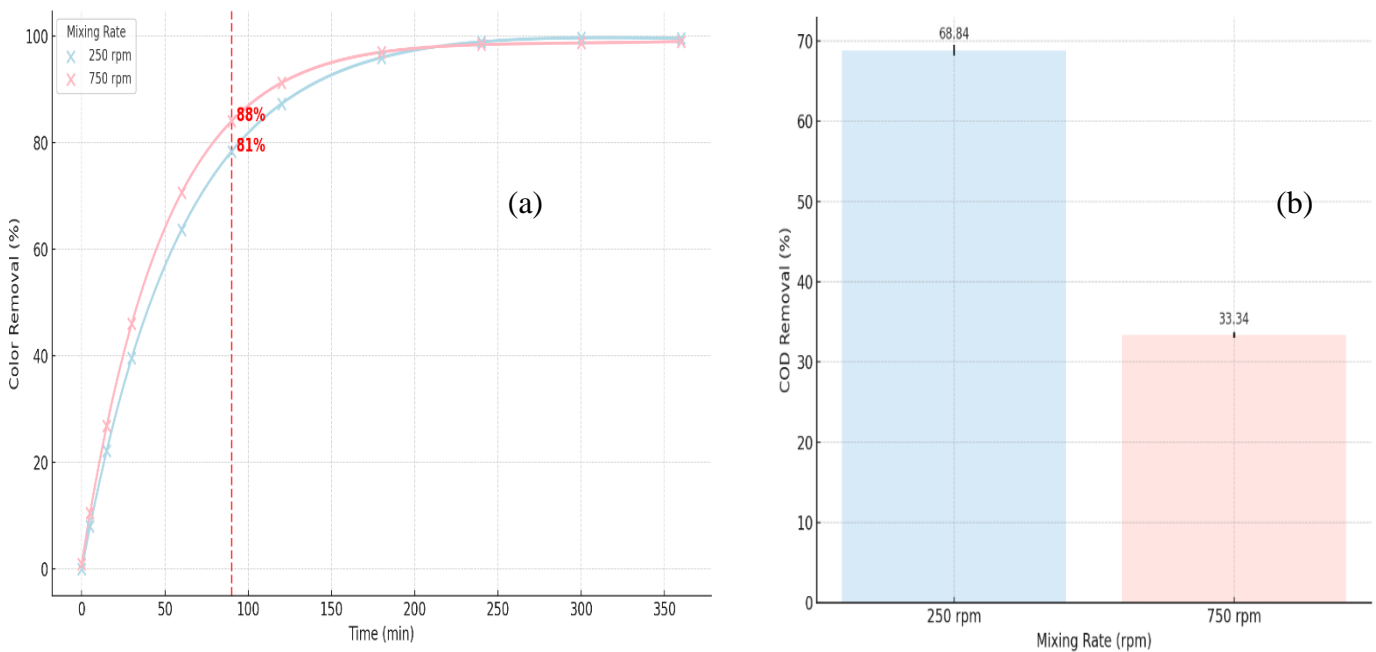


**Figure IV.5:** Effect of the mixing rate on color and COD removal. (a): Effect of the mixing rate on color removal. (b): Effect of the mixing rate on COD removal. The COD obtained is at 360 minutes.

A mixing rate of 250 rpm was selected for further experimentation, as it provided an effective compromise between adequate mass transfer and mechanical stability. This mixing rate contributed to enhanced contact between pollutants and reactive species without introducing excessive turbulence, given that this condition ensures optimal energy use by combining low energy consumption (EC) with high current efficiency (CE), as illustrated in Fig IV.6, while a mixing rate of 750 rpm showed inefficient energy usage marked by high EC, low CE, and consequently higher operational costs.

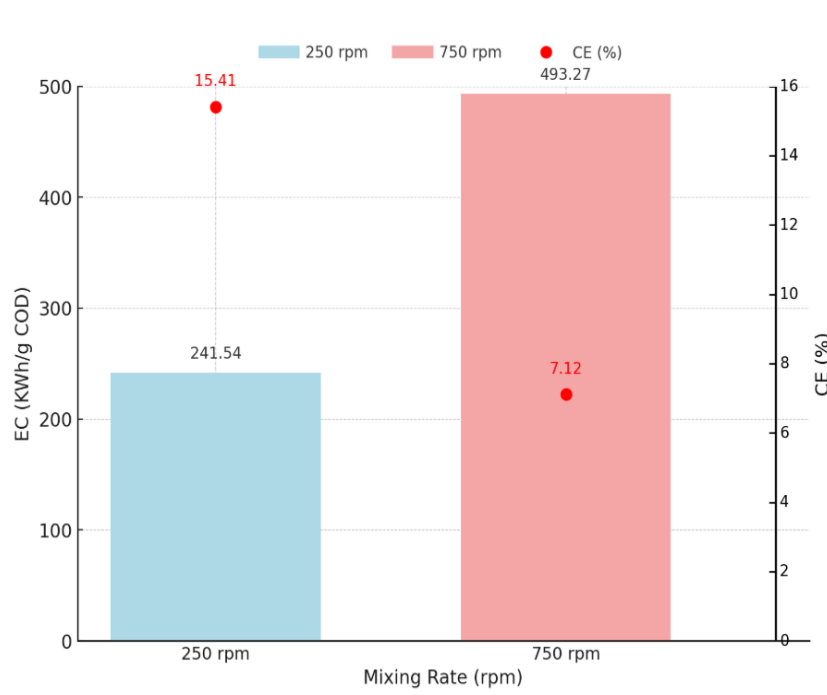


**Figure IV.6:** The energy consumption and current efficiency for the electrodes at different mixing rates. Bars correspond to EC and dots correspond to CE.

## IV.5 Effect of the concentration of methylene blue on color and COD removal

The effect of initial methylene blue (MB) concentration on electrochemical oxidation efficiency was evaluated using the boron-doped diamond (BDD) electrode. The experiments were conducted under the final chosen parameters, selected for yielding the best performance: an inter-electrode distance of 0.5 cm, a current intensity of 0.06 A/cm<sup>2</sup>, and a stirring speed of 250 rpm. Methylene blue solutions were prepared at 50 ppm and 200 ppm for testing.

### IV.5.1 Effect of the concentration of methylene blue on color removal

At 50 ppm, complete color removal was achieved  $100.00 \pm 0.00$ , indicating an exceptionally consistent and highly effective decolorization process. This reflects the strong oxidative power of the BDD electrode under moderate dye load, where the available oxidizing species are sufficient to fully break down chromophoric structures.

At 200 ppm, color removal reached  $92.77\% \pm 0.02$  (95% CI: [92.73, 92.81]). While still high, this represents a clear reduction compared to the 50 ppm condition. The low standard deviation confirms that the process remained reproducible, but the drop in performance suggests that the higher dye concentration begins to strain the oxidative capacity of the system.

This may lead to incomplete breakdown of chromophores due to competition for available reactive species, Fig IV. 7(a).

Similar studies have shown that at low initial dye concentrations, the generation of reactive oxygen species, hydroxyl radicals ( $\bullet\text{OH}$ ), is sufficient to attack and degrade chromophoric structures effectively, resulting in rapid color removal, as seen by Panizza et al. [125], who used a boron-doped diamond (BDD) anode to degrade synthetic dyes. The favorable oxidant-to-dye ratio at low concentrations allows for high decolorization efficiency. Consequently, when the initial concentration is increased, the removal efficiency of color decreases due to the limited generation of reactive species relative to the increased molecular load, as seen by Chou et al. [126]. Additionally, the rise in solution turbidity at higher concentrations hinders electron transfers and limit the mass transfer to the electrode surface, further limiting the reaction kinetics and color removal efficiency.

#### **IV.5.2 Effect of the concentration of methylene blue on COD removal**

In terms of mineralization, a notable difference was observed between the two concentrations.

At 50 ppm, COD removal reached  $80.96 \pm 0.03$  (95% CI: [80.76, 81.16]) corresponding to 66.71mg  $\text{O}_2/\text{L}$ , reflecting excellent reproducibility and high mineralization efficiency, taking into note that with an initial COD value of 373.22 mg $\text{O}_2/\text{L}$ . This indicates that under moderate dye loading, the generation of hydroxyl radicals and other reactive species by the BDD anode is sufficient not only to remove color but also to effectively degrade organic matter.

At 200 ppm, COD removal dropped significantly to  $42.28 \pm 0.02$  (95% CI: [42.19, 42.37]) corresponding to 409,17 mg $\text{O}_2/\text{L}$  at the end, taking into note that with an initial COD value of 712.26 mg $\text{O}_2/\text{L}$ . Despite remaining highly reproducible, this substantial decrease demonstrated that the higher organic load exceeded the oxidative capacity of the system. The limited availability of oxidizing species relative to the increased pollutant concentration led to less effective mineralization, even though color removal remained high. These results confirm that COD removal efficiency decreases as methylene blue concentration increases, reinforcing the importance of maintaining a balanced pollutant load to ensure optimal electrochemical performance, Fig IV. 7(b).

Previous experimental studies and research have also shown that low initial dye concentrations facilitate more effective COD removal, as the reduced organic load allows for

the complete mineralization of pollutants into carbon dioxide and water, as seen by Rathinakumaran et al. [127]. Under these conditions, the reactive species generated at the electrode surface are preferentially consumed in deep oxidation reactions, leading to a more efficient breakdown of complex organics and the lower organic load ensures that reactive species are directed toward complete oxidation rather than forming stable intermediates minimizing their accumulation. Prior findings also revealed that at higher initial concentrations, COD removal becomes less efficient due to the formation and persistence of refractory oxidation intermediates and insufficient oxidant availability to sustain full mineralization, as seen by Chou et al. [126]. The process kinetics shifts to a mass transport-limited process, wherein the degradation rate is controlled by the diffusion of pollutants rather than the kinetics of the electrochemical reaction itself, which further impairs removal efficiency and increases energy consumption per unit of COD degraded.

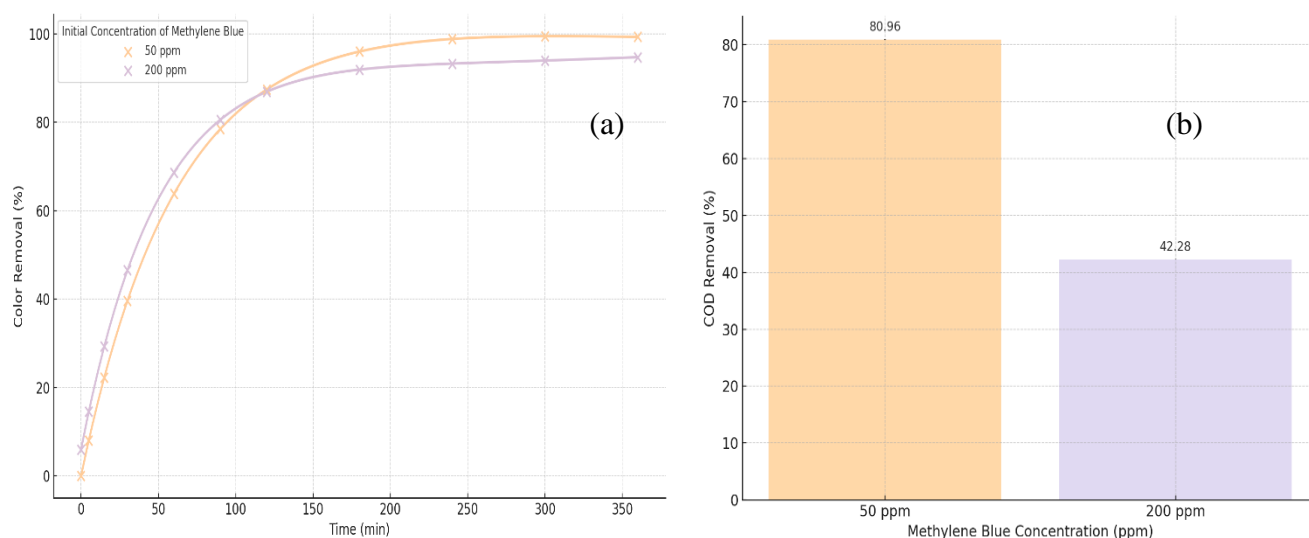


**Figure IV. 7:** Effect of the initial concentration of methylene blue on color and COD removal. (a): Effect of the initial concentration of methylene blue on color removal. (b): Effect of the initial concentration of methylene blue on COD removal. The COD obtained is at 360 minutes.

This study confirmed that the initial concentration of methylene blue plays a crucial role in determining the efficiency of both color and COD removal during electrochemical treatment with BDD electrodes. These findings highlight that while BDD electrodes ensure efficient and consistent decolorization across concentrations, higher initial dye concentrations compromise

COD removal, emphasizing the need to optimize the initial pollutant load for effective electrochemical treatment, given the fact that lower initial concentrations favor improved color and COD removal performance, and under these conditions, energy use is optimized through lower energy consumption (EC) and high current efficiency (CE), as depicted in Fig IV.8, whereas higher initial concentrations exhibit poor energy utilization, with elevated EC, reduced CE, and increased operational costs.

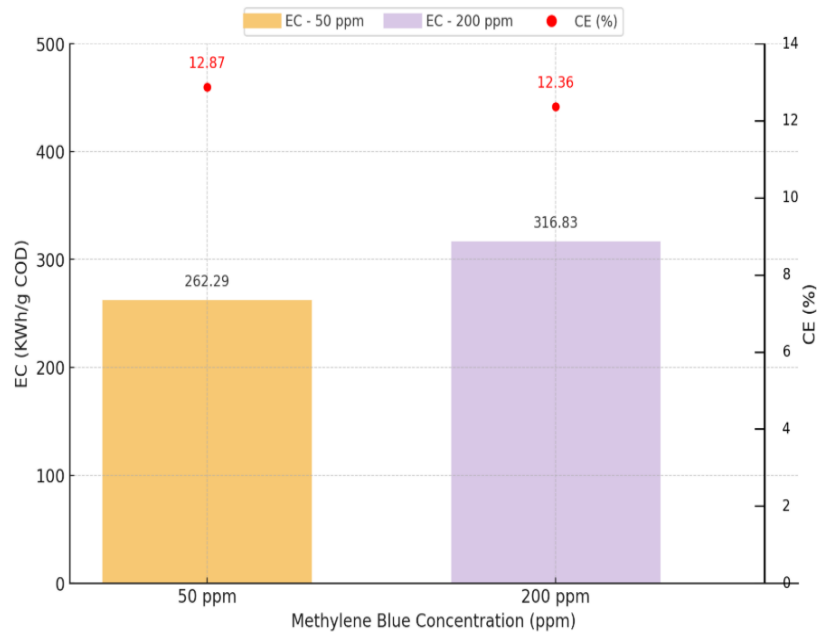


**Figure IV.8:** The energy consumption and current efficiency at different initial methylene blue concentrations. Bars correspond to EC and dots correspond to CE.

## **CHAPTER V**

# **CONCLUSIONS AND PERSPECTIVES**

This study demonstrated that electrolytic oxidation is an effective and sustainable method for treating textile wastewater, achieving significant removal of both color and chemical oxygen demand (COD) under optimized conditions. The research focused on the influence of multiple operational parameters, including anode material, current density, inter-electrode distance, mixing rate, and initial dye concentration. The findings emphasize the promising potential of this advanced oxidation process for addressing the persistent challenge in treating industrial wastewater.

The anodes tested in this study were boron-doped diamond (BDD), titanium with ruthenium dioxide coating (Ti/RuO<sub>2</sub>), and titanium with iridium dioxide coating (Ti/IrO<sub>2</sub>). Among these, BDD emerged as the most efficient, demonstrating superior performance in pollutant degradation and color removal. This anode delivered the highest COD reduction and complete color removal, highlighting its strong oxidizing capability and electrochemical stability, indicating BDD's enhanced reactivity and greater ability to reduce methylene blue content and COD levels.

The study also assessed the impact of current density, revealing that a value of 0.06 A/cm<sup>2</sup> was optimal striking a balance between low and high current regimes by delivering high pollutant removal efficiencies. This intermediate current density proved sufficient to sustain the continuous generation of oxidative species without leading to excessive energy consumption.

Furthermore, the inter-electrode distance significantly influenced electrochemical performance. A shorter distance of 0.5 cm resulted in better treatment outcomes due to increased electric field strength and reduced ohmic resistance, allowing for better transfer of oxidizing agents throughout the solution.

The mixing rate also affected treatment efficiency. A rate of 250 rpm was more favorable as it maintained stable hydrodynamic conditions, minimized flow irregularities, and reduced the impact of ohmic losses, thereby supporting uniform electrochemical reactions. In contrast, 750 rpm introduced excessive flow disturbances that negatively impacted current distribution and reactive species utilization.

As the final parameter studied, the initial dye concentration was found to significantly affect removal efficiency. Lower concentrations, such as 50 ppm, led to enhanced outcomes by minimizing the saturation of active sites on the electrode surface and ensuring more effective interaction between the pollutants and generated oxidants. Maintaining a controlled initial dye concentration is thus essential for achieving reliable and reproducible electrochemical treatment results.

In summary, these findings highlight the effectiveness of electrolytic oxidation in achieving complete color removal and high COD reduction, successfully addressing the treatment of synthetic textile wastewater through a high-performance and environmentally sustainable process.

This study provides valuable insights into electrochemical oxidation methods that can enhance the treatment of textile wastewater, benefiting both environmental protection efforts and guiding future applications in industrial settings by emphasizing the importance of optimal operational conditions for effective color and COD removal.

The findings from this study highlight the influence of electrode material, current density, inter-electrode distance, mixing rate, and initial dye concentration on treatment efficiency for the development of an efficient electrochemical treatment system.

This perspective emphasizes how scientific research can directly impact environmental engineering, potentially leading to new standards in electrochemical reactor design and operational protocols. This research also opens the discussion for innovation in sustainable wastewater treatment technologies, demonstrating how interdisciplinary approaches integrating electrochemistry can offer comprehensive solutions to water pollution challenges.

## References

[1] Dang M., Deng Q.-L., Tian Y.-Y., Liu C., Shi H.-P., Fang G.-Z., et al. (2020). Synthesis of anionic ionic liquids@TpBd-(SO<sub>3</sub>)<sub>2</sub> for the selective adsorption of cationic dyes with superior capacity. *RSC Adv.* 10(9):5443-53.

Available at <https://doi.org/10.1039/C9RA10035K>

[2] Crini G. (2005). Non-conventional low-cost adsorbents for dye removal: a review. *Bioresource Technology.* 97(9):1061-85.

Available at <https://doi.org/10.1016/j.biortech.2005.05.001>

[3] Zhang Y., Wang Q., Li R., Lou Z., Li Y. (2020). A novel phenolic foam-derived magnetic carbon foam treated as adsorbent for Rhodamine B: characterization and adsorption kinetics. *Crystals.* 10(3):159.

Available at <https://doi.org/10.3390/cryst10030159>

[4] Natarajan R., Manivasagan R. (2019). Effect of operating parameters on dye wastewater treatment using *Prosopis cineraria* and kinetic modeling. *Environmental Engineering Research.* 25(5):788-93.

Available at <https://doi.org/10.4491/eer.2019.308>

[5] Inglezakis V.J., Pouloupoulos S.G. (2006). Adsorption, Ion Exchange and Catalysis: Design of Operations and Environmental Applications.

Available at <https://doi.org/10.1016/B978-0-444-52783-7.X5000-9>

[6] Martínez-Huitle C.A., Ferro S. (2006). Electrochemical oxidation of organic pollutants for the wastewater treatment: direct and indirect processes. *Chem. Soc. Rev.* 35:1324–1340.

Available at <https://doi.org/10.1039/B517632H>

[7] Britto J.M., Rangel M.C. (2008). Advanced oxidation processes of phenolic compounds in industrial effluents 31:114–122.

Available at <https://doi.org/10.1590/S0100-40422008000100023>

[8] Särkkä H., Bhatnagar A., Sillanpää M., (2015). Recent developments of electro-oxidation in water treatment, a review. *J. Electroanalytical. Chemistry.* 754:46–56.

Available at <https://doi.org/10.1016/j.jelechem.2015.06.016>

[9] Parshetti P. (2023). Electrochemical degradation and mineralization of organic dyes in aqueous nitrate solutions. *Chemosphere.* Volume 316.

Available at <https://doi.org/10.1016/j.chemosphere.2023.137821>

[10] Foroutan I. (2023). Electrochemical degradation and mineralisation of organic dyes in aqueous nitrate solution. *Chemosphere.* Volume 316.

Available at <https://doi.org/10.1016/j.chemosphere.2023.137821>

[11] Mukimin A., Hanny H., Nani N., Nanik I.S., Djayanti S., Astuti Y., (2024). Electrochemical reactor and system as post-treatment of textile wastewater. *Journal of Water Process Engineering* Volume 59.

Available at <https://doi.org/10.1016/j.jwpe.2024.105028>

[12] Sudarshan S., Harikrishnan S., Rathi Bhuvaneswari G., Alamelu V., Aanand S., Rajasekar A., Govarthanam M. (2023). Impact of textile dyes on human health and bioremediation of textile industry effluent using microorganisms: current status and future prospects. NCBI.

Available at DOI: [10.1093/jambio/lxac064](https://doi.org/10.1093/jambio/lxac064)

[13] European Parliament and Council of the European Union. (2000). Off. J. Eur. Commun. L327/.

[14] “Directive 2000/60/EC. Water Framework Directive, European Commission”.

[15] Brillas E., Martínez-Huitle C.A. (2015). Decontamination of wastewaters containing synthetic organic dyes by electrochemical methods. *Catal. B: Environ.* 166-167:603-643.

Available at <https://doi.org/10.1016/j.apcatb.2014.11.016>

[16] Chen C., Lu C. (2007). Photocatalytic degradation of basic violet 4: degradation efficiency, product distribution and mechanisms. *J. Phys. Chem. C* 111:13922-13932.

Available at <https://doi.org/10.1021/jp0738964>

[17] Tung C.-H., Shen S.-Y., Chang J.-H., Hsu Y.-M., Lai Y.-C. (2013). Treatment of real printing wastewater with an electro-catalytic process. *Sep. Purif. Technol.* 117:131–136.

Available at <https://doi.org/10.1016/j.seppur.2013.07.028>

[18] Zhou X.J., Guo W.Q., Yang S.S., Ren N.Q. (2012). A rapid and low energy consumption method to decolorize the high concentration triphenylmethane dye wastewater: operational parameters optimization for the ultrasonic-assisted ozone oxidation process. *Bioresour Technol.* NIH,105:40–47.

Available with DOI [10.1016/j.biortech.2011.11.089](https://doi.org/10.1016/j.biortech.2011.11.089)

[19] Basha C.A., Sendhil J.S., Kumar K., Muniswaran P.K.A., Lee C.W. (2012). Electrochemical degradation of textile dyeing industry effluent in batch and flow reactor systems. *Desalination* 285 :188–197.

Available at <https://doi.org/10.1016/j.desal.2011.09.054>

[20] Li X., Wang C., Qian Y., Wang Y., Zhang L. (2013). Simultaneous removal of chemical oxygen demand, turbidity and hardness from biologically treated citric acid wastewater by electrochemical oxidation for reuse. *Sep. Purif. Technol.* 107:281-288.

Available with DOI [10.1016/j.seppur.2013.01.008](https://doi.org/10.1016/j.seppur.2013.01.008)

[21] Singh S., Srivastava V.C., Mandal T.K. (2015). Treatment of fertilizer industry wastewater by catalytic peroxidation process using copper-loaded SBA-15. *J. Environ. Sci. Health A.* NIH, 50:1468-1478.

Available with DOI [10.1080/10934529.2015.107448](https://doi.org/10.1080/10934529.2015.107448)

[22] Mondal B., Srivastava V.C., Kushwaha J.P., Bhatnagar R., Singh S., Mall I.D. (2013). Parametric and multiple response optimizations for the electrochemical treatment of textile printing dye-bath effluent. *Sep. Purif. Technol.* 109:135–143.

Available at <https://doi.org/10.1016/j.seppur.2013.02.026>

[23] Singh S., Srivastava V.C., Mall I.D., (2014). Electrochemical treatment of dye bearing effluent with different anode–cathode combinations: mechanistic study and sludge analysis. *Ind. Eng. Chem. Res.* 53:10743–10752.

Available at <https://doi.org/10.1021/ie4042005>

[24] Katheresan V., Kansedo J., Lau S.Y., (2018). Efficiency of various recent wastewater dye removal methods: A review. *Journal of Environmental Chemical Engineering*. ;6(4):4676-97

Available with DOI [10.1016/j.jece.2018.06.060](https://doi.org/10.1016/j.jece.2018.06.060)

[25] Akbari A., Remigy J.C., Aptel P., (2002). Treatment of textile dye effluent using a polyamide-based nanofiltration membrane. *Chem. Eng. Process*.41:601–609.

Available at [https://doi.org/10.1016/S0255-2701\(01\)00181-7](https://doi.org/10.1016/S0255-2701(01)00181-7)

[26] Adegoke K.A., Bello O.S., (2015). Dye sequestration using agricultural wastes as adsorbents. *Water Resources and Industry*; 12:8-24.

Available at <https://doi.org/10.1016/j.wri.2015.09.002>

[27] Barışçı S., Turkay O., Dimoglo A., (2016). Review on greywater treatment and dye removal from aqueous solution by ferrate (VI). *Ferrites and Ferrates: Chemistry and Applications in Sustainable Energy and Environmental Remediation*:349-409.

Available with DOI: [10.1021/bk-2016-1238.ch014](https://doi.org/10.1021/bk-2016-1238.ch014)

[28] dos Santos A.B., Cervantes F.J., Lier J.B.V., (2007). Review paper on current technologies for decolourisation of textile wastewaters: perspectives for anaerobic biotechnology. *Bioresource. Technology*. 98(12):2369–2385.

Available at <https://doi.org/10.1016/j.biortech.2006.11.013>

[29] Ballav N., Das R., Giri S., (2018). L-cysteine doped polypyrrole (Ppy@L-cyst): a super adsorbent for the rapid removal of Hg<sup>2+</sup> and efficient catalytic activity of the spent adsorbent for reuse. *Chemical Engineering Journal*. 345:621–630.

Available at <https://doi.org/10.1016/j.cej.2018.01.093>

[30] Mojsov K.D., Gaber S., (2016). The application of enzymes for the removal of dyes from textile effluents. *Advanced Technology*. 5(1):81–86.

Available with DOI: [10.5937/savteh1601081M](https://doi.org/10.5937/savteh1601081M)

[31] Sahari N.S., Shahir S., Ibrahim A., Hasmoni S.H., Altowayti W.A.H., (2023). Bacterial nanocellulose and its application in heavy metals and dyes removal. NIH.

Available at <https://pubmed.ncbi.nlm.nih.gov/37814051/>

[32] Mojsov K.D., Andronikov D., Janevski A., Kuzelov A., Gaber S., (2016). The application of enzymes for the removal of dyes from textile effluents. *Advanced technologies*,5(1):81-6.

Available with DOI: [10.5937/savteh1601081M](https://doi.org/10.5937/savteh1601081M)

[33] Katheresan V., Kandedo J., Lau S.Y., (2018). Efficiency of various recent wastewater dye removal methods: A review. *Journal of Environmental Chemical Engineering*,6(4):4676-97

Available with DOI: [10.1016/j.jece.2018.06.060](https://doi.org/10.1016/j.jece.2018.06.060)

[34] Baddouh K., (2023). Electrochemical degradation and mineralisation of organic dyes in aqueous nitrate solutions. *Chemosphere Volume 316*.

Available at <https://doi.org/10.1016/j.chemosphere.2023.137821>

[35] Jovi'c, Sarfo D.K., Kaur A., Marshall D.L., Anthony P., O'Mullane A.P., (2023). Electrochemical degradation and mineralisation of organic dyes in aqueous nitrate solutions. *Chemosphere Volume 316*.

Available at <https://doi.org/10.1016/j.chemosphere.2023.137821>

[36] Robinson T., McMullan G., Marchant R., Nigam P., (2001). Remediation of dyes in textile effluent: a critical review on current treatment technologies with a proposed alternative. *Bioresour. Technol.*77:247–255.

Available at [https://doi.org/10.1016/S0960-8524\(00\)00080-8](https://doi.org/10.1016/S0960-8524(00)00080-8)

[37] Forgacs E., Cserháti T., Oros G., (2004). Removal of synthetic dyes from wastewaters: a review. *Environ. Int.* 30:953–971.

Available at <https://doi.org/10.1016/j.envint.2004.02.001>

[38] Moreira F.C., Boaventura R., Brillas E., Vilar V.J.P., (2017). Electrochemical advanced oxidation processes: a review on their application to synthetic and real wastewaters. *Appl Catal B Environ*, 202:217–261.

Available at <https://doi.org/10.1016/j.apcatb.2016.08.037>

[39] Garcia-Segura S., Lanzarini-Lopes M., Hristovski K., Westerhoff P., (2018). Electrocatalytic reduction of nitrate: fundamentals to full-scale water treatment applications. *Appl Catal B Environ*, 236.

Available at <https://doi.org/10.1016/j.apcatb.2018.05.041>

[40] Martínez-Huitle C.A., Rodrigo M.A., Sirés I., Scialdone O., (2015). Single and coupled electrochemical processes and reactors for the abatement of organic water pollutants: a critical review. *Chem Rev*, 115:13362–13407.

Available at <https://doi.org/10.1021/acs.chemrev.5b00361>

[41] Radjenovic J., Sedlak D.L., (2015). Challenges and opportunities for electrochemical processes as next-generation technologies for the treatment of contaminated water. *Environ Sci Technol*, 49:11292–11302.

Available at <https://doi.org/10.1021/acs.est.5b02414>

[42] Wenzel T., (2023). Basic concepts in electrochemistry. *Analytical Sciences Digital Library*.

Available at

[https://chem.libretexts.org/Bookshelves/Analytical\\_Chemistry/Supplemental\\_Modules\\_\(Analytical\\_Chemistry\)/Analytical\\_Sciences\\_Digital\\_Library/In\\_Class\\_Activities/Electrochemical\\_Methods\\_of\\_Analysis/02\\_Text/1.\\_Basic\\_Concepts\\_in\\_Electrochemistry](https://chem.libretexts.org/Bookshelves/Analytical_Chemistry/Supplemental_Modules_(Analytical_Chemistry)/Analytical_Sciences_Digital_Library/In_Class_Activities/Electrochemical_Methods_of_Analysis/02_Text/1._Basic_Concepts_in_Electrochemistry)

[43] Garg A., Mishra I.M., Chand S., (2005). Thermochemical precipitation as a pre-treatment step for the chemical oxygen demand and color removal from pulp and paper mill effluent. *Ind. Eng. Chem. Res.* 44:2016–2026.

Available at <https://doi.org/10.1021/ie048990a>

[44] Kushwaha J.P., Srivastava V.C., Mall I.D., (2011). Studies on electrochemical treatment of dairy wastewater using aluminum electrode. *AIChE J.* 57:2589–2598.

Available at <https://doi.org/10.1002/aic.12463>

[45] Singh S., Srivastava V.C., Mandal T.K., Mall I.D., (2013). Multistep optimization and residue disposal study for electrochemical treatment of textile wastewater using aluminum electrode. *Int. J. Chem. Reactor Eng.* 11:1–16.

Available with DOI: [10.1515/ijcre-2012-0019](https://doi.org/10.1515/ijcre-2012-0019)

[46] Martinez-Huitle C.A., Ferro S., (2006). Electrochemical oxidation of organic pollutants for the wastewater treatment: direct and indirect processes. *Chem. Soc. Rev.* 35:1324–1340.

Available at <https://doi.org/10.1039/B517632H>

[47] Panizza M., Cerisola G., (2009). Direct and mediated anodic oxidation of organic pollutants. *Chem. Rev.* 109:6541–6569.

Available at <https://doi.org/10.1021/cr9001319>

[48] Martinez-Huitle C.A., Quiroz M.A., Comninellis C., Ferro S., Battisti A., (2004). Electrochemical incineration of chloranilic acid using Ti/IrO<sub>2</sub>, Pb/PbO<sub>2</sub> and Si/BDD electrodes. *Electrochimica Acta.* 50:949–956.

Available at <https://doi.org/10.1016/j.electacta.2004.07.035>

[49] Martinez-Huitle C.A., Ferro S., Battisti A., (2005). Electrochemical incineration in the presence of halides. *Electrochem. Solid-State Lett.* 8:D35–D39.

Available with DOI [10.1149/1.2042628](https://doi.org/10.1149/1.2042628)

[50] Panizza M., Cerisola G., (2008). Electrochemical degradation of methyl red using BDD and PbO<sub>2</sub> anodes. *Ind. Eng. Chem. Res.* 47:6816–6820.

Available with DOI : [10.1021/ie8001292](https://doi.org/10.1021/ie8001292)

[51] Martinez-Huitle C.A., Brillas E., (2009). Decontamination of wastewaters containing synthetic organic dyes by electrochemical methods: a general review. *Appl. Catal. B: Environ.* 8:105–145.

Available at <https://doi.org/10.1016/j.apcatb.2008.09.017>

[52] Ferro S., Martinez-Huitle C.A., Battisti A., (2010). Electrooxidation of oxalic acid at different electrode materials. *J. Appl. Electrochem.* 40:1779–1787.

Available with DOI: [10.1007/s10800-010-0113-y](https://doi.org/10.1007/s10800-010-0113-y)

[53] Sires I., Brillas E., Oturan M.A., Rodrigo M.A., Panizza M., (2014). Electrochemical advanced oxidation processes: today and tomorrow: A review. *Environ. Sci. Pollut. Res.* 21:8336–8367.

Available with DOI: [10.1007/s11356-014-2783-1](https://doi.org/10.1007/s11356-014-2783-1)

[54] Subramanyan V., Oturan M.A., (2014). Electrochemistry: as cause and cure in water pollution—an overview. *Environ. Chem. Lett.* 12:97–108.

Available with DOI: [10.1155/2010/232378](https://doi.org/10.1155/2010/232378)

[55] Pillai M.I.S., Gupta A.K., (2015). Potentiostatic electrodeposition of a novel cost-effective PbO<sub>2</sub> electrode: Degradation study with emphasis on current efficiency and energy consumption. *J. Electroanal. Chem.* 749:16–25.

Available with DOI: <https://doi.org/10.1016/j.jelechem.2015.04.020>

[56] Pillai M.I.S., Gupta A.K., (2015). Batch and continuous flow anodic oxidation of 2, 4-dinitrophenol: Modeling, degradation pathway, and toxicity. *J. Electroanal. Chem.* 756:108–117.

Available at: <https://doi.org/10.1016/j.jelechem.2015.08.020>

[57] Lipsa S., (2020). Electrochemical method—concept, types, and electrochemical cells.

Available with DOI: DOI:[10.13140/RG.2.2.21520.43522](https://doi.org/10.13140/RG.2.2.21520.43522)

[58] Chaudhary N., Khanuja M., (2022). Electrochemistry - Concepts and methodologies. (31-50)

Available at <https://doi.org/10.1016/B978-0-12-823148-7.00002-7>

[59] Brillas E., Martínez-Huitle C.A., (2015). Decontamination of wastewaters containing synthetic organic dyes by electrochemical methods. *Appl. Catal. B: Environ.* 166–167:603–643.

Available at <https://doi.org/10.1016/j.apcatb.2014.11.016>

[60] Garcia-Segura S., Anotai J., Singhadech S., Lu M-C, (2017). Enhancement of biodegradability of o-toluidine effluents by electroassisted photo-Fenton treatment. *Process Saf. Environ. Protect.* Volume 106. (60-67)

Available at <https://doi.org/10.1016/j.psep.2016.12.011>

[61] Brillas E., Martínez-Huitle C.A., (2015). Decontamination of wastewaters containing synthetic organic dyes by electrochemical methods. An updated review. *Appl. Catal. B: Environ.* 166–167:603–643.

Available at <https://doi.org/10.1016/j.apcatb.2014.11.016>

[62] Basha A.C., Chithra E., Sripriyalakshmi, N.K., (2009). Electro-degradation and biological oxidation of non-biodegradable organic contaminants. *Chem. Eng. J.* 149:25–34.

Available at <https://doi.org/10.1016/j.cej.2008.09.037>

[63] Cai J., Zhou M., Liu Y., Savall A., Groenen S.K., (2018). Indirect electrochemical oxidation of 2,4-dichlorophenoxyacetic acid using electrochemically-generated persulfate. *Chemosphere*, 204:163–169.

Available at <https://doi.org/10.1016/j.chemosphere.2018.04.004>

[64] Pérez J.F., Llanos J., Sáez C., López C., Cañizares P., Rodrigo M.A., (2017). Treatment of real effluents from the pharmaceutical industry: a comparison between Fenton oxidation and conductive diamond electro-oxidation. *J. Environ. Manag.* 195:216–223.

Available with DOI: [10.1016/j.jenvman.2016.08.009](https://doi.org/10.1016/j.jenvman.2016.08.009)

[65] Martínez-Huitle C.A., Ferro S., (2006). Electrochemical oxidation of organic pollutants for wastewater treatment: direct and indirect processes. *Chem. Soc. Rev.* 35:1324–1340.

Available at <https://doi.org/10.1039/B517632H>

[66] Panizza M., Cerisola G., (2009). Direct and mediated anodic oxidation of organic pollutants. *Chem. Rev.* 109:6541–6569.

Available at <https://doi.org/10.1021/cr9001319>

[67] Matzek S., (2023). Electrochemical degradation and mineralisation of organic dyes in aqueous nitrate solutions. *Chemosphere* 316.

Available with DOI: [10.1016/j.chemosphere.2023.137821](https://doi.org/10.1016/j.chemosphere.2023.137821)

[68] Iniesta J., Michaud P.A., Panizza M., Cerisola G., Aldaz A., Comninellis C., (2001). Electrochemical oxidation of phenol at boron-doped diamond electrode. *Electrochim. Acta* 46:3573–3578.

Available at [https://doi.org/10.1016/S0013-4686\(01\)00630-2](https://doi.org/10.1016/S0013-4686(01)00630-2)

[69] Chen X., Chen G., Gao F., Yue P.L., (2003). High-performance Ti/BDD electrodes for pollutant oxidation. *Environ. Sci. Technol.* 37:5021–5026.

Available at <https://doi.org/10.1021/es026443f>

[70] Cañizares P., Martínez L., Paz R., Sáez C., Lobato J., Rodrigo M.A., (2006). Treatment of Fenton-refractory olive oil mill wastes by electrochemical oxidation with boron-doped diamond anodes. *J. Chem. Technol. Biotechnol.* 81:1331–1337.

Available at <https://doi.org/10.1002/jctb.1428>

[71] Cañizares P., Lobato J., Paz R., Rodrigo M.A., Sáez C., (2006). Advanced oxidation processes for the treatment of olive-oil mill wastewater. *Chemosphere* 67:832–838.

Available at <https://doi.org/10.1016/j.chemosphere.2006.10.064>

[72] Zhu X., Shi X., Wei J., (2007). The electrochemical oxidation of phenol on boron-doped diamond and Ti/SnO<sub>2</sub>-Sb<sub>2</sub>O<sub>5</sub> electrodes. *Water Res.* 41:654–660.

Available with DOI : [10.1016/S0013-4686\(01\)00630-2](https://doi.org/10.1016/S0013-4686(01)00630-2)

[73] Kraft A., Stadelmann M., Blaschke M., (2003). Anodic oxidation with doped diamond electrodes: a new advanced oxidation process. *J. Hazard. Mater.* 103:247–261.

Available at <https://doi.org/10.1016/j.jhazmat.2003.07.006>

[74] Koparal A.S., Yildiz Y.S., Keskinler B., Demircioglu N., (2007). Effect of initial pH on the removal of humic substances from wastewater by electrocoagulation. *Sep. Purif. Technol.* 52:280–287.

Available with DOI: [10.1016/j.seppur.2007.06.004](https://doi.org/10.1016/j.seppur.2007.06.004)

[75] Ganiyu S.O., Martinez-Huitle C.A., Oturan M.A., (2019). Electrochemical advanced oxidation processes for wastewater treatment: advances in reactor design and electrode materials. *Curr. Opin. Electrochem.* 16:83–90.

Available with DOI: [10.1016/j.coelec.2020.100678](https://doi.org/10.1016/j.coelec.2020.100678)

[76] Comninellis C., Pulgarin C., (1993). Electrochemical oxidation of phenol for wastewater treatment using SnO<sub>2</sub> anodes. *J. Appl. Electrochem.* 23:108–112.

Available with <https://doi.org/10.1590/S0104-66322012000400008>

[77] Boudenne J.L., Cerclier O., Galéa J., Van der Vlist E., (1996). Electrochemical oxidation of aqueous phenol at a carbon black slurry electrode. *Appl. Catal. A Gen.* 143:185–202.

Available at [https://doi.org/10.1016/0926-860X\(96\)00027-0](https://doi.org/10.1016/0926-860X(96)00027-0)

[78] Tahar N.B., Savall A., (1999). A comparison of different lead dioxide coated electrodes for the electrochemical destruction of phenol. *J. New Mater. Electrochem. Syst.* 2:19–26.

Available with DOI: [10.1007/s10800-007-9442-x](https://doi.org/10.1007/s10800-007-9442-x)

[79] Chen X., Chen G., Yue P.L., (2003). Anodic oxidation of dyes at novel Ti/B-diamond electrodes. *Chem. Eng. Sci.* 58:995–1001.

Available at [https://doi.org/10.1016/S0009-2509\(02\)00640-1](https://doi.org/10.1016/S0009-2509(02)00640-1)

[80] Gotsi M., Kalogerakis N., Psillakis E., Samaras P., Mantzavinos D., (2005). Electrochemical oxidation of olive oil mill wastewaters. *Water Res.* 39:4177–4187.

Available at <https://doi.org/10.1016/j.watres.2005.07.037>

[81] Belaid C., Kallel M., Khadhraou M., Lalleve G., Elleuch B., Fauvarque J.F., (2006). Electrochemical treatment of olive mill wastewaters: removal of phenolic compounds and decolourization. *J. Appl. Electrochem.* 36:1175–1182.

Available at [https://doi.org/10.1016/S1001-0742\(12\)60037-0](https://doi.org/10.1016/S1001-0742(12)60037-0)

[82] Panizza M., Cerisola G., (2006). Olive mill wastewater treatment by anodic oxidation with parallel plate electrodes. *Water Res.* 40:1179–1184.

Available at <https://doi.org/10.1016/j.watres.2006.01.020>

[83] Giannis A., Kalaitzakis M., Diamadopoulos E., (2007). Electrochemical treatment of olive mill wastewater. *J. Chem. Technol. Biotechnol.* 82:663–671.

Available with DOI: [10.1002/jctb.1725](https://doi.org/10.1002/jctb.1725)

[84] Kotta E., Kalogerakis N., Mantzavinos D., (2007). The effect of solids on the electrochemical treatment of olive mill effluents. *J. Chem. Technol. Biotechnol.* 82:504–511.

Available at <https://doi.org/10.1002/jctb.1706>

[85] Un U.T., Altay U., Koparal A.S., Ogutveren U.B., (2008). Complete treatment of olive mill wastewaters by electrooxidation. *Chem. Eng. J.* 139:445–452.

Available at <https://doi.org/10.1016/j.cej.2007.08.009>

[86] Chatzisyneon E., Dimou A., Mantzavinos D., Katsaounis A., (2009). Electrochemical oxidation of model compounds and olive mill wastewater over DSA electrodes: 1. the case of Ti/IrO<sub>2</sub> anode. *J. Hazard. Mater.* 167:268–274.

Available with DOI: [10.1016/j.jhazmat.2008.12.117](https://doi.org/10.1016/j.jhazmat.2008.12.117)

[87] Papastefanakis N., Mantzavinos D., Katsaounis A., (2010). DSA electrochemical treatment of olive mill wastewater on Ti/RuO<sub>2</sub> anode. *J. Appl. Electrochem.* 40:729–737.

Available with DOI: [10.1007/s10800-009-0050-9](https://doi.org/10.1007/s10800-009-0050-9)

[88] Comninellis C., Vercesi G.P., (1991). Characterization of DSA-type oxygen evolving electrodes: choice of a coating. *J. Appl. Electrochem.* 21:335–345.

Available at <https://doi.org/10.1007/BF01020219>

[89] Baroud M., Chraibi A., Gherbi A., Cherkaoui R., Benkhalti F., Krouti M., Gherbi A. (2025). Revealing the Surface and In-Depth Operational Performances of Oxygen-Evolving Anode Coatings: A Guideline for the Synthesis of Inert Durable Anodes in Metal Electrowinning from Acid Solutions. *Journal of the Electrochemical Society* 172(1), 014502.

Available at <https://doi.org/10.3390/met14121339>

[90] Martinez-Huitle C.A., Ferro S., (2006). Electrochemical oxidation of organic pollutants for the wastewater treatment: direct and indirect processes. *Chem. Soc. Rev.* 35:1324–1340.

Available at <https://doi.org/10.1039/B517632H>

[91] Panizza M., Cerisola G., (2009). Direct and mediated anodic oxidation of organic pollutants. *Chem. Rev.* 109:6541–6569.

Available at <https://doi.org/10.1021/cr9001319>

[92] Panizza M., Cerisola G., (2003). Electrochemical oxidation of 2-naphthol with in situ electrogenerated active chlorine. *Electrochem. Acta* 48:1515–1519.

Available at [https://doi.org/10.1016/S0013-4686\(03\)00028-8](https://doi.org/10.1016/S0013-4686(03)00028-8)

[93] White G.C., (1999). Handbook of Chlorination. John Wiley & Sons, New York.

Available at <https://doi.org/10.1021/ja9956932>

[94] Tavares M.G., Da Silva L.V.A., Solano A.M.S., Tonholo J., Martinez-Huitle C.A., Zanta C.L.P.S., (2012). Electrochemical oxidation of methyl red using Ti/Ru<sub>0.3</sub>Ti<sub>0.7</sub>O<sub>2</sub> and Ti/P anodes. Chem. Eng. J. 204–206:141–150.

Available with DOI: [10.1016/j.cej.2012.07.056](https://doi.org/10.1016/j.cej.2012.07.056)

[95] Kumar S., Singh S., Srivastava V., (2015). Electro-oxidation of nitro-phenol by ruthenium oxide coated titanium electrode: Parametric, kinetic and mechanistic study. Chem. Eng. J. 263:135–143.

Available at <https://doi.org/10.1016/j.cej.2014.11.051>

[96] Zhang Y., Wang X., He J., Zhang Z., (2021). Advances in the development of titanium-based anodes for electrochemical water treatment. Chemosphere 282:131064.

Available at <https://doi.org/10.1039/C6EE01807F>

[97] Patake V.D., Lokhande C.D., (2010). RuO<sub>2</sub>/Co<sub>3</sub>O<sub>4</sub> thin films prepared by spray pyrolysis technique for supercapacitors Journal of Solid State Electrochemistry 14(7):1205-1211.

Available with DOI: [10.1007/s10008-009-0955-6](https://doi.org/10.1007/s10008-009-0955-6)

[98] Audichon T., Morisset S., (2014). Electroactivity of RuO<sub>2</sub>–IrO<sub>2</sub> mixed nanocatalysts toward the oxygen evolution reaction in a water electrolyzer supplied by a solar profile. International Journal of Hydrogen Energy 39(30):16785–16796.

Available with DOI: [10.1016/j.ijhydene.2014.07.170](https://doi.org/10.1016/j.ijhydene.2014.07.170)

[99] Yaqub A., Isa M., Ajab H., Junaid M., (2017). Preparation of Ti/TiO<sub>2</sub> anode for electrochemical oxidation of toxic priority pollutants. J. New Mater. Electrochem. Syst. 20:7–12.

Available at <https://doi.org/10.14447/jnmes.v20i1.287>

[100] Yaqub A., Isa M., Ajab H., Kutty S., Ezechi E., (2017). Polycyclic aromatic hydrocarbons removal from produced water by electrochemical process optimization. *Ecol. Chem. Eng. S.* 24(3):397–404.

Available at <https://doi.org/10.1016/j.hazadv.2023.100388>

[101] Li X., Cui Y., Feng Y., Xie Z., Gu J., (2005). Reaction pathways and mechanisms of the electrochemical degradation of phenol on different electrodes. *Water Res.* 39:1972–1981.

Available at <https://doi.org/10.1016/j.watres.2005.02.021>

[102] Chen G., (2004). Electrochemical technologies in wastewater treatment. *Sep. Purif. Technol.* 38:11–41.

Available at <https://doi.org/10.1016/j.seppur.2003.10.006>

[103] Yao J., Zhou M., Wen N., Xue W., Wang D., (2016). Electrochemical conversion of ammonia to nitrogen in non-chlorinated aqueous solution by controlling pH value. *J. Electroanal. Chem.* 776:53–58.

Available at <https://doi.org/10.1016/j.jelechem.2016.06.040>

[104] Zhu R.Y., Yang C.Y., Zhou M., Wang D., (2015). Industrial park wastewater deeply treated and reused by a novel electrochemical oxidation reactor. *Chem. Eng. J.* 260:427–433.

Available at <https://doi.org/10.1016/j.cej.2014.09.029>

[105] « Diário da República - 1 Série-A, Ministério do Ambiente, Decreto-Lei n.º 236/98, de 1 de Agosto ».

[106] “ISO 10523:2008 - Water quality - Determination of pH.”

[107] “ISO 7888:1985 - Water Quality - Determination of Electrical Conductivity. “

[108] “ISO 17025:2017 - General requirements for the competence of testing and calibration laboratories.”

[109] Garg V. K., Gupta R., Bala M., (2021). Advanced oxidation processes for dye removal from industrial wastewater: A review. *Environmental Technology & Innovation*, 24, 101853.

Available with DOI [10.4018/978-1-7998-0311-9.ch010](https://doi.org/10.4018/978-1-7998-0311-9.ch010)

[110] “ISO 8245:2013 - Water quality - Guidelines for the determination of total organic carbon (TOC) and dissolved organic carbon (DOC)”

[111] Wang J., Xu L., (2022). Comparison of aerobic and anaerobic treatment methods for COD removal in wastewater treatment plants. *Water Research*, 218, 118503.

Available with DOI: [10.1007/978-981-10-4130-3\\_4](https://doi.org/10.1007/978-981-10-4130-3_4)

[112] Körbahti B, Turan K. Evaluation of Energy Consumption in Electrochemical Oxidation of Acid Violet 7 Textile Dye Using Pt/Ir Electrodes. *Journal of the Turkish Chemical Society, Section A: Chemistry*. 2016;3(3):75–92.

Available with DOI: [10.18596/jotcsa.31804](https://doi.org/10.18596/jotcsa.31804)

[113] “ISO 5725:1994 - Accuracy of measurement methods and Results-General principles and definitions. ”

[114] Bensalah N., Abdel-Wahab A., (2020). Electrochemical Treatment of synthetic and Actual Dyeing Wastewaters Using BDD Anodes. *BioOne digital library*.

Available at <https://doi.org/10.1177/ASWR.S3639>

[115] Sadia Khan S., Tayyaba N., Naseem I., Yaqub L., Photocatalytic Dye Degradation from Textile Wastewater: A Review, Volume 9, Issue 20.

Available at <https://doi.org/10.1021/acsomega.4c00887>

[116] Xinhui X., Fengyi Z., Jianju L., Haizhou Y., Liangliang W., Qiaoyang L., Junqiu J., Guangshan Z., Qingliang Z., (2020). A Review Study on Sulfate-Radical-Based Advanced Oxidation Processes for Domestic/Industrial Wastewater Treatment: Degradation, Efficiency, and Mechanism.

Available with DOI [10.3389/fchem.2020.592056](https://doi.org/10.3389/fchem.2020.592056)

[117] Koparal A., Ogutveren U., (2013). Fluoride removal from water and wastewater with a batch cylindrical electrode using electrocoagulation. *Chemical Engineering Journal*, 223:110–115.

Available at <https://doi.org/10.1016/j.cej.2013.02.126>

[118] Aljaberi Y., Mohammed W., (2018). Adsorption of lead from simulated wastewater via electrocoagulation process: kinetics and isotherm studies.

Available at

[https://www.researchgate.net/publication/324312799\\_Adsorption\\_of\\_lead\\_from\\_simulated\\_wastewater\\_via\\_electrocoagulation\\_process\\_kinetics\\_and\\_Isotherm\\_Studies](https://www.researchgate.net/publication/324312799_Adsorption_of_lead_from_simulated_wastewater_via_electrocoagulation_process_kinetics_and_Isotherm_Studies)

[119] Jiachao Y., Mei Y., Junhui J., Guanghua X., Jun C., (2022). Process Optimization of Electrochemical Treatment of COD and Total Nitrogen Containing Wastewater. National Library of Medicine.

Available at <https://doi.org/10.3390/ijerph19020850>

[120] Sastrawidana I., Sukarta D.,(2018). Indirect Electrochemical Oxidation with Multi Carbon Electrodes for Restaurant Wastewater Treatment. *Journal of Ecological Engineering*, 19(1), 195–199.

Available at <https://doi.org/10.12911/22998993/79414>

[121] Phan H., Hoan N., Huy N., Duc N., Anh N., (2021),Effect of Current and Electrodes Area to Color Removal Efficiency and Energy Consumption by Electrocoagulation Process, Sustainable Development of Water and Environment (169-179).

Available with DOI: [10.1007/978-3-030-75278-1\\_16](https://doi.org/10.1007/978-3-030-75278-1_16)

[122] Thella K., Verma B., Srivastava V., Srivastava K., (2008). Impact of electrode distance on removal efficiency in electrochemical dye treatment. *J. Environ. Sci. Health, Part A* 43(5):554–562.

Available at <https://doi.org/10.1080/10934520801889815>

[123] Khandegar V., Saroha A., (2013). Electrochemical treatment of textile effluent containing acid dye. *J. Environ. Manage.* 128:949–963.

Available at <https://doi.org/10.1016/j.jenvman.2013.06.012>

[124] Bannari, A. (2006). Turbulence intensity in an electrochemical cell: Effect on reactor performance. *Chemical Engineering and Processing: Process Intensification*, 45(6), 471–480.

Available at <https://doi.org/10.1016/j.cep.2005.11.002>

[125] Panizza, M., & Cerisola, G. (2008). Electrochemical oxidation of 2-naphthol with synthetic BDD anode. *Electrochimica Acta*, 53(3), 2289–2295.

Available at: <https://doi.org/10.1016/j.electacta.2007.09.031>

[126]. Chou, W. L., Wang, C. T., Chang, C. Y., & Kuo, Y. M. (2011). Electrochemical degradation of dye wastewater using a paired cell reactor with a Ti/RuO<sub>2</sub> anode and an electro-Fenton cathode. *Desalination*, 271(1–3), 55–61.

Available at : <https://doi.org/10.1016/j.desal.2010.12.009>

[127] Rathinakumaran, S., & Meyyappan, R. M. (2015). Electrochemical degradation of textile dye wastewater using mixed oxide-coated DSA electrodes: kinetic and energy analysis. *Environmental Progress & Sustainable Energy*, 34(4), 1021–1029.

Available at : <https://doi.org/10.1002/ep.12045>